Cross-Scale: Multi-scale Coupling in Space Plasmas
ESA Cosmic Vision 2015-2025 Call for Proposals

The Cross-Scale Team

28 June 2007

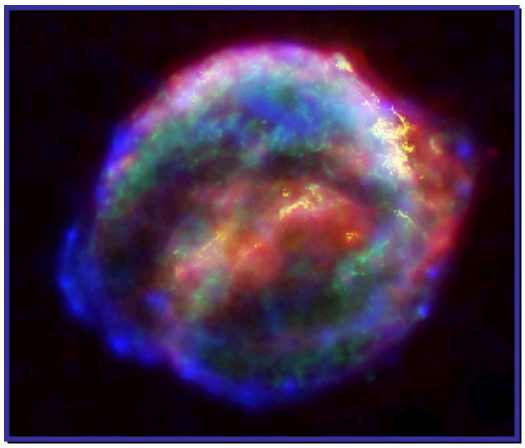

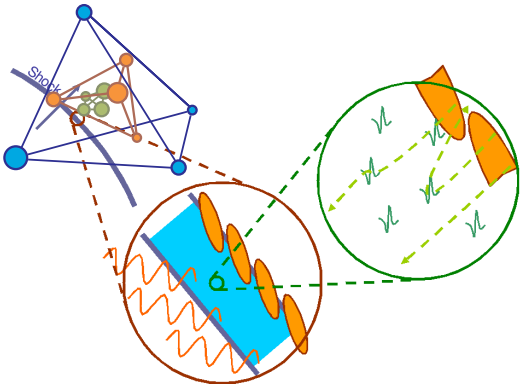

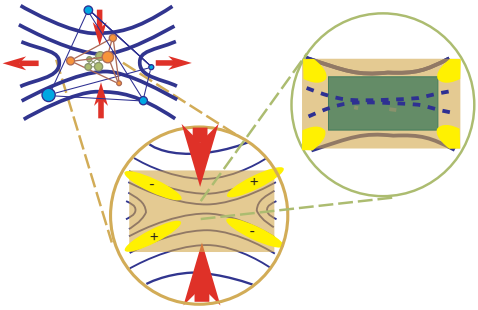

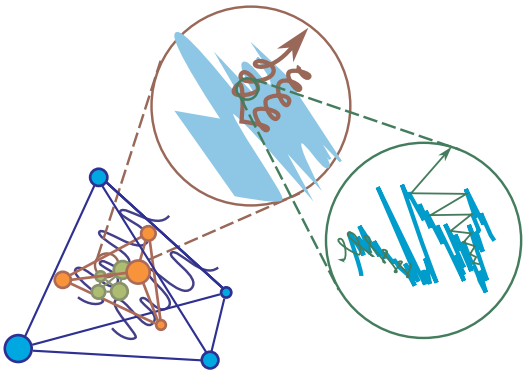

Contact Prof. Steven J. Schwartz, Blackett Laboratory, Imperial College London, London SW7 2AZ, UK. Tel: +44 (0)20 7594 7660; Fax: +44 (0)20 7594 7772; email: s.schwartz@imperial.ac.uk.

Contents

1 Executive Summary

Most of the visible universe is in the highly ionised plasma state, and most of that plasma is collisionfree. Plasma processes are at work everywhere, from radio galaxy jets and supernova explosions to solar flares and planetary magnetospheres. Cross-Scale is an M-class mission dedicated to quantifying the coupling in plasmas between different physical scales. This cross-scale coupling, being highly variable and structured, is critical in underpinning and quantifying the physical mechanisms inferred in plasmas that are difficult to observe.

As plasma regimes encounter each other, the absence of collisions raises fundamental questions about how energy is shared amongst the three main elements (electrons, ions, and overall bulk flows). These constituents, each of which operates on its own physical scale, are coupled through electromagnetic fields.

Three fundamental physical processes operate to bring about the universal collisionless plasma coupling in physical environments where momentum and energy transfer is important.

Shock waves guide strong flows around obstacles or at interfaces between two flow regimes. They are important locations for the transfer of directed bulk flow energy into heat, with an attendant acceleration of energetic particles.

Magnetic reconnection releases stored magnetic energy to the plasma, and allows for exchange of material between previously isolated regions. Moreover, the consequent change in magnetic topologies provides a coupling between plasma regions which often drives the global scale dynamics of the system.

Turbulence transports energy from large scales at which it is input to small scales where it is dissipated. In the process, it interacts strongly, and often selectively, with plasma particle populations as either a source or sink (or both) of energy.

Near-Earth space is a unique laboratory for quantifying the physics of these three processes. Breakthroughs have arisen due to the high quality of data that, unlike more distant regimes, is sampled directly by plasma and fields experiments on satellites.

To date, in situ measurements have focused on terrestrial phenomena, such as the mechanisms that populate the van Allen belts. Dual spacecraft studies during the 1980's began to address the real microphysics. Present generation missions (Cluster and MMS) utilise 4 spacecraft to sample a specific volume, and hence characterise the physics operating on the single scale corresponding to the spacecraft separation. By the time MMS has flown, we shall have a catalogue of behaviour that ranges from the smallest, electron scale, to the largest fluid-like phenomena.

That knowledge is incomplete due to the ambiguity and uncertainty about the dynamics and variability of the larger contextual scales (for the electron and ion scales) and of the internal microprocesses that mediate the energy exchange (for the larger scales). The complex, dynamic nonlinear coupling of scales and physical mechanisms can not be quantified without *simultaneous* information on all scales.

Cross-Scale will target compelling and fundamental questions, such as: How do shocks accelerate and heat particles? How does reconnection convert magnetic energy? How does turbulence control transport in plasmas? These address directly the Cosmic Vision question "How does the Solar System work?" by studying basic processes occurring "From the Sun to the edge of the Solar System." Moreover, by quantifying the fundamental plasma processes involved, the advances made by the mission will extend beyond the Solar System to plasmas elsewhere in the Universe.

Cross-Scale will employ 10 spacecraft which will fly with two highly complementary spacecraft from its sister mission SCOPE provided by JAXA. Together, they will form three nested tetrahedra to separate spatial and temporal variations simultaneously on the three key scales for the first time.

The spacecraft, which carry a minimal payload with strong heritage, will be launched into a highly elliptical Earth orbit. Over the two year mission they will encounter various collisionless shocks, explore regions of both spontaneous and strongly driven reconnection, and investigate both nascent and highly evolved plasma turbulence.

There are no technologies that need to be developed or proven for a launch in 2017, or earlier. The mission is thus low risk for high science return. It taps directly into European leadership in multipoint in situ space plasmas. This proposal is signed by researchers from around the world.

In the pages that follow, we amplify the universal science objectives and present a mature, concrete mission concept that fully meets these objectives.

2 Scientific Objectives

2.1 Universal Plasma Processes

A small number of phenomena dominate the behaviour and effects of plasmas throughout the Universe: collisionless shocks, magnetic reconnection and plasma turbulence. Shock waves resulting from supernova explosions and other energetic flows accelerate cosmic rays to high energies. Magnetic reconnection plays a pivotal role in the release of stored energy in phenomena as diverse as solar flares and γ-ray-rich "magnetars." Turbulence in astrophysical disks allows accretion to proceed by transporting angular momentum; it also channels energy from the largest scales through a cascade to the smallest where it dissipates.

2.1.1 Shocks

Shock waves are formed whenever a supersonic flow encounters an obstacle of some kind, including other material. The basic process involves a transition from supersonic to subsonic flow, so that information can propagate sufficiently upstream of the obstacle to deflect the oncoming flow. To do so, a shock must decelerate, deflect, compress, and heat the incident material. Classically, the shock transition occurs abruptly, on scales related to the dissipative (i.e., collisional) processes.

In astrophysical contexts, however, the incident material is usually a highly ionised plasma in which collisions are negligibly rare. Under these circumstances, shock waves may still exist, but the absence of collisional coupling can result in highly non-equilibrium physics that can be traced to the multiple scales associated with multiple species and fields.

Collisionless plasma shocks are some of the most spectacular, visually striking and energetic events in the Universe. Generated by supernovae, stellar winds, or the rapid motion of objects such as neutron stars, they have a number of important effects. Supernova shock waves trigger the collapse of galactic nebulae and hence the formation of planetary systems. They are responsible for heating and deflecting the surrounding plasma, and blow large-scale magnetic bubbles out of galactic disks. Collisionless shocks also accelerate particles to extraordinarily high energies.

The interaction of the fast-moving solar wind with the Earth's magnetosphere results in a bowshock. Its curvature means that regions of quasi-parallel (magnetic field parallel to the shock normal) and quasi-perpendicular shock front co-exist, and that the Mach number varies across the shock surface. Magnetohydrodynamic Mach numbers can reach 20, comparable to those in many astrophysical scenarios. The terrestrial bowshock is therefore a useful analogue for astrophysical shocks. The ability to measure particle distributions and electromagnetic fields around and within the shock front makes it possible to study the details of the collisionless shock transition and accompanying non-thermal phenomena. Historically, in situ measurements at the bow shock and interplanetary shocks have challenged existing theory and led to significant advances in computational modelling.

2.1.2 Reconnection

Magnetic reconnection is a fundamental plasma physics process which breaks down the barriers between neighbouring plasmas, releasing energy from their magnetic fields, transferring material and momentum between those plasmas, and accelerating a part of the plasma population to high energies.

The Universe is filled with situations where reconnection is expected to play significant roles in their dynamical evolution, including stars (exotic and otherwise) and planetary systems at all stages of their life cycles. Reconnection also governs the interactions of those systems with their surrounding media.

In highly electrically conductive space plasmas, the constituent charged particles are unable to convect transverse to the local magnetic field direction; the magnetic flux is "frozen in" to the plasma material. Thus two such plasmas in regions of magnetic flux with different sources generally cannot mix. They are separated by a sheet of electrical current that exerts the forces acting to keep the plasmas apart. The plasmas remain isolated from one another, even if pressed together by external forces or momentum. However, exceptions to this principle arise in situations in which magnetic reconnection occurs.

A key consequence of magnetic reconnection is the linkage of magnetic fields from the two neighbouring plasmas, allowing material to flow between the previously isolated regions (e.g., from a stellar atmosphere to planetary magnetosphere or between different regions of the solar corona - see Figure 1). The reconnection process locally disrupts the current sheet, changes the topology of the

Case Study: SLAMS and Particle Acceleration: A universal shock process in operation

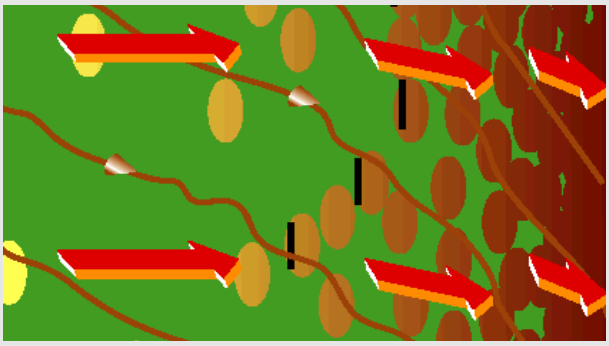

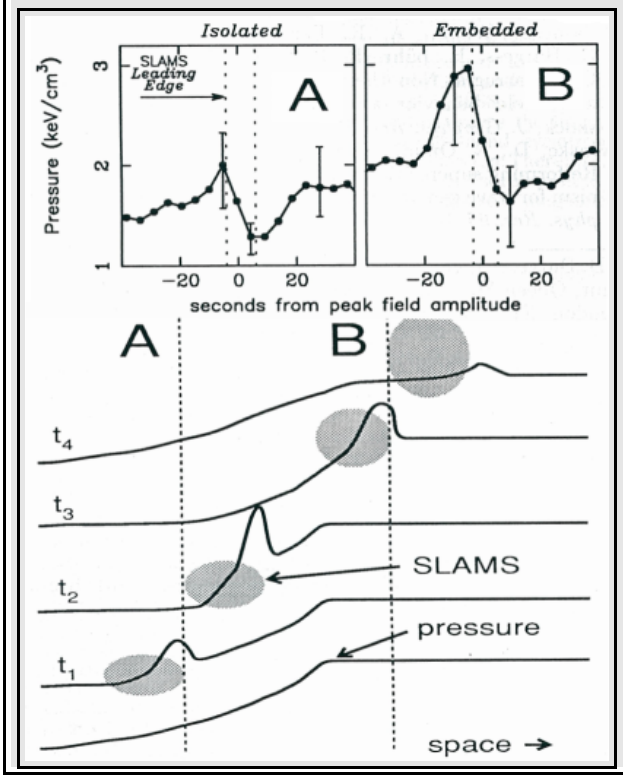

The quasi-parallel shock transition, (left) as envisaged in early work (after [1]) based on limited multi-spacecraft data. Studies showed that the coherent Short Large Amplitude Magnetic Structures (SLAMS) sweep up suprathermal particles (bottom left, from [2]) during the acceleration process, in contrast to the traditional picture of diffusive first-order Fermi acceleration with monotonic pressure profiles.

More recent results shown below at 1/10th (top) and 1/100th (bottom) of the dimension inferred from[1], reveal considerable sub-structure, calling into question some of the key assumptions about the scales associated with shocks and Fermi acceleration under quasi-parallel conditions. The variability and small-scale structure has important, and to date elusive, implications for the efficiency of the quasi-parallel shock in terms of energy partition and ion acceleration. (after [3, 4]).

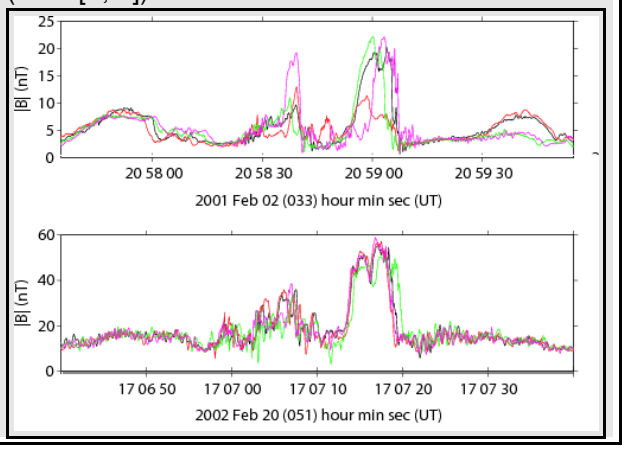

magnetic fields, and releases its energy, e.g., into the bulk flow and heat of the plasma.

Many in situ measurements made by spacecraft at current sheets in the vicinity of Earth (principally the magnetopause and the magnetotail current sheet) have provided compelling evidence that reconnection does indeed occur in collisionless space plasmas. However, these have yet to provide clear indications of how it happens or a complete picture of what conditions are needed to initiate and maintain the process. For example, observations suggest that a necessary, but not sufficient, condition for sustained magnetic reconnection is a significant shear angle between the magnetic field vectors in the two adjacent plasma regions. Processes occurring on much smaller scales, comparable to ion and probably even electron gyroradii, appear to play a key role in initiating and supporting reconnection. In turn, these localised processes result in global scale consequences for the dynamics of the plasma systems. Thus to understand the way or ways in which reconnection arises, operates, and controls large scale dynamics, it is essential that we investigate the process across all relevant scales.

2.1.3 Turbulence

Turbulence is present in many astrophysical plasmas such as the interstellar medium, accretion disks, the solar wind, supernova remnants, and collapsing nebulae. It is also dynamically important in the transport of energy, mass and momentum in

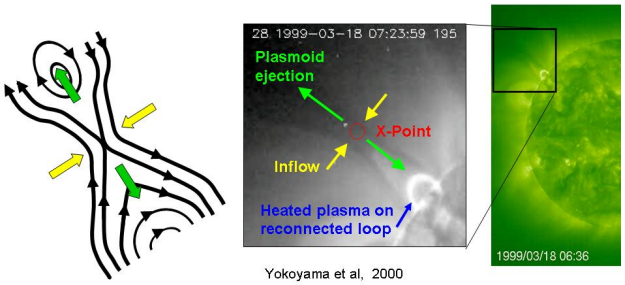

Figure 1: The image on the right shows a reconnection event occurring in the Sun's corona. A study by Yokoyama et al.[5] identified coronal plasma in- and outflowing (yellow and green arrows) as expected for a reconnection event, as well as heated material appearing on closed magnetic loops formed by reconnection.

many of these environments. The accurate prediction of turbulent properties, and their effects on the surrounding plasma, is therefore key to the quantitative analysis of many astrophysical scenarios, as well as terrestrial plasmas such as tokamaks.

Measurements of turbulence in solar system plasmas have provided several key insights into its behaviour which are difficult or impossible to obtain any other way: the scaling of the main energy cascade, anisotropy, spatial variability, and effects on particle propagation and energisation. Recently, multi-spacecraft techniques have made it possible to uniquely identify energised wave modes, offering a revolution in our ability to analyse plasma turbulence. Such advances both validate and challenge theoretical and numerical models.

Despite these successes, many key questions remain unanswered concerning the nature of the turbulent cascade, particularly near the ion and electron kinetic scales: How is it driven to an anisotropic state by the magnetic field and its local environment? How does it spontaneously generate structures from a previously uniform plasma? These issues must all be quantified if the large scale effects of space plasma turbulence are to be predicted.

2.1.4 Multi-scale Coupling

Shocks, reconnection, and turbulence are controlled by dynamics which are coupled on 3 fundamental scales simultaneously: electron kinetic, ion kinetic, and fluid. It is the nonlinear interaction of 3D, time-varying structures on these 3 scales which produces the complex behaviour and consequences of these processes. Critically, most astrophysical plasmas are collisionless, which means that their constituents can be far from equilibrium with each other. The resulting nonlinear dynamics provides diverse and exotic mechanisms for momentum and energy flow and redistribution.

The complex, three dimensional nature of plasma structures has long been recognised. Previous, existing and upcoming missions have been designed to measure this 3D structure using multiple spacecraft. A minimum of four spacecraft are necessary to determine 3D structure: ESA's Cluster and NASA's upcoming MMS missions both use four spacecraft for this task. A fundamental restriction of multi-spacecraft measurements, however, is that they are sensitive to scales of the order of the spacecraft separation. With four spacecraft, multiple scales can be probed by varying this separation, but only one scale can be measured at any time.

Plasmas are not just three dimensional: they also contain time-varying structure on many scales, simultaneously. Different scales are affected by different physical processes. It is the interplay of these which results in the complexity of shocks, reconnection, and other phenomena, and consequently in their large scale effects.

To understand the interplay of forces and dynamics within such regions and hence predict their effects, it is essential to measure the time-dependent behaviour in 3D on the three key physical scales – electron, ion and fluid. This can only be achieved with spacecraft positioned such that some have separations comparable to each of these three physical scales, simultaneously. Thus 4 spacecraft are required at each of the three physical scales, making a complement of 12 spacecraft in total. Instrumentation on the spacecraft at each scale must be tailored to the physical processes at that scale. Near-Earth space, which is relatively accessible and contains examples of all the phenomena of interest, is the obvious target for such a mission, which we call Cross-Scale.

While simulations of collisionless plasmas have revealed a great deal about their dynamics and complexity, it is not possible to simulate the key phenomena of interest in sufficiently large simulation boxes to resolve the three logarithmically-spaced physical scales in 3D. Indeed, this goal will not be achieved within the time scale of ESA's Cosmic Vision 2015-2025 programme, assuming that computer power increases at its historical rate. Neither can laboratory plasmas be probed over the

Table 1: Cross-Scale main science questions and multi-scale coupling physics

How do shocks accelerate and heat particles?
How do shocks accelerate particles?
coherent magnetic structures; surface ripples
How is the energy incident on a shock partitioned?
ion reflection; cross-shock potential; electron demagnetisation
How do shock variability and reformation influence shock acceleration?
response to upstream variability; non-steady reformation
How does reconnection convert magnetic energy?
What initiates magnetic reconnection?
non-adiabatic particle motion; dissipation of boundary current
How does the magnetic topology evolve?
Hall currents; current sheet tearing; magnetic island coalescence; magnetic tension
How does reconnection accelerate particles and heat plasma?
parallel electric field; perpendicular drifts; wave electric fields
How does turbulence control transport in plasmas?
How does the turbulence cascade transfer energy across physical scales?
ion & electron dissipation scales; wavemode identification
How does the magnetic field break the symmetry of plasma turbulence?
magnetic field braiding; effect of boundaries
How does turbulence generate coherent structures?
ion & electron instabilities; intermittency

necessary scales. The only way to validate theoretical concepts and limited numerical experiments concerning these phenomena, and so to study them in sufficient detail, is to measure them directly in space.

In the following subsections we describe in more detail the specific science questions relating to shocks, magnetic reconnection, and turbulence. These set the science objectives in their present context and understanding, highlight the important areas where there are crucial uncertainties, and reveal how Cross-Scale measurements will replace doubt and qualitative concepts with a definitive and quantifiable framework.

2.2 How do shocks accelerate and heat particles?

Cross-scale coupling is integral to shocks in collisionless plasmas. Small scale electron dynamics results in a highly structured, fluctuating electric field within the shock ramp. At scales around an order of magnitude larger, ions gyrate through the ramp, with trajectories determined by the fluctuating electric field. Reflected and gyrating ions then generate the even larger scale reformation and rippling of the shock front, which in turn affects the small scale dynamics of the electrons - as well as being pivotal in the acceleration of inflowing particles to high energies.

Collisionless shocks both heat the main plasma constituents and accelerate sub-populations of ions and electrons to high energies. This acceleration is possible because the physics involves more than one scale. Acceleration is a part of the larger question about how shocks partition the bulk flow energy incident upon them, which again is effected over fluid, ion, and electron scales. Finally, variations in the flow that drives them, and instabilities within the transition scales, leads to transient phenomena that can significantly alter or enhance the

acceleration efficiency.

2.2.1 How do shocks accelerate particles?

Diffusive acceleration

Some particles are reflected from the shock. Their propagation into the upstream plasma is unstable to the generation of waves, which in turn scatter them – a highly nonlinear process. This initiates further acceleration. However, many aspects of this process are poorly understood, and involve spatially variable structures, both within the shock and in the upstream plasma.

Fundamental to modern acceleration theory is the scattering length of the energised particles. Repeated reflection and scattering (the so-called "first order Fermi" process) can accelerate particles to very high energies. Recent studies[6] have for the first time evaluated the scattering mean free path for shock-accelerated particles. Simultaneous measurements of the resonant plasma waves and particles over ion and fluid scales is required to quantify the wave modes and particle interactions over a range of plasma conditions. Only in this way can we predict shock acceleration efficiencies in other astrophysical environments.

Coherent acceleration

The surface of shocks is believed to be rippled by local ion and current instabilities, but the properties of these ripples, e.g., amplitude and wavelength, are unknown. The ripples provide time-varying fields which can trap some particles, enabling them to "surf" the shock front and systematically pick up energy from the large-scale motional electric field. Such surfing is potentially important for both ion and electron acceleration, and may "inject" suprathermal particles into the first order Fermi process, the efficiency of which is dramatically improved if fed a pre-accelerated population. In order to quantify the effects of shock ripples, simultaneous measurements are required of ripples of the shock surface at fluid scales; of ion distribution variations around and within the ripples, with variations on the scale of an ion gyroradius; and of electron heating and acceleration at the smallest scales.

Quasi-parallel shocks are associated with Short Large Amplitude Magnetic Structures (SLAMS) which grow in the generally turbulent foreshock/shock region accompanied by energetic particles. Their polarisation suggests they grow due to a hot ion instability, essentially feeding off the particle pressure gradients, whereas other foreshock turbulence is beam-driven. Thus the relationship between SLAMS and the general turbulence is not clear. The basic presumed structure is sketched in the Case Study on page 4.

Again, the origin and evolution of the cycle of turbulence and particles needs to be explored by measurements at the disparate scales. SLAMS exhibit internal structure down to electron scales, and their overall size, shape and porosity are correspondingly difficult to determine without multi-scale observations. Yet these characteristics are critical to our picture of quasi-parallel shocks. Large scale measurements of the orientation of SLAMS, energetic particle gradients and foreshock waves must be combined with ion-scale structures within SLAMS, with electron-scale fine structure, and with 3D electric field measurements.

2.2.2 How is the energy incident on a shock partitioned?

In the frame of the shock, the upstream, incoming plasma carries kinetic, thermal and electromagnetic energy into the shock front. This energy is then partitioned into a number of forms. Most is distributed between the downstream kinetic and thermal energies of the ions and electrons. Knowledge of the fraction of energy distributed into each of these plasma constituents is essential for predicting the large scale effects of shocks. For example, the energy taken up by electron heating, together with the actual shape of electron energy spectra, at astrophysical shocks is responsible for the observed X-ray emission. It is possible to measure this partitioning directly at the terrestrial bowshock. However, this does not mean that the physical processes by which the redistribution of energy occurs are well known. Indeed, this partitioning varies considerably with shock parameters and is also highly variable in space and time, so the application of these measurements to astrophysical shocks is not straightforward without a detailed knowledge of the physical processes which govern the energy distribution.

Ion reflection

The rise in electric potential through the shock layer is responsible for decelerating the incoming ions, some of which are reflected at shocks above a critical Mach number. This reflection initiates the spread in velocities that will ultimately account for

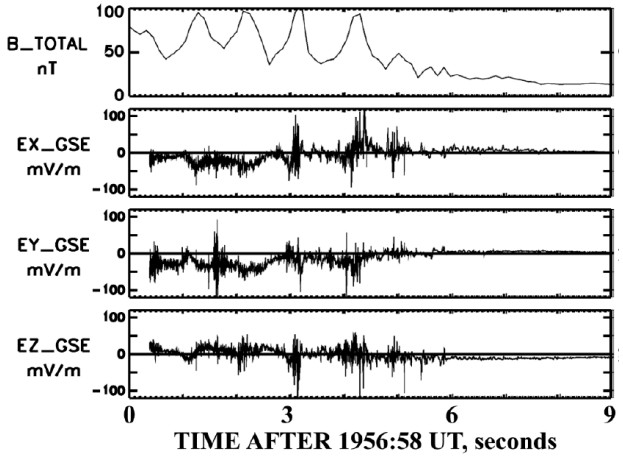

Figure 2: Recent measurements of the 3D electric field at a high-Mach number collisionless shock which reveal the presence of electric field spikes (lower panels) on scales much smaller than the ion scale variation in the magnetic field shown in the top panel. The size and variability of such spikes is not known. Full 3D measurements at multiple scales are required to transform such electric fields into the cross-shock electric potential that controls both the ion and electron dynamics. (from [8])

the rise in non-directed motion (the "heating" required of the shock).

However, the potential is the integral of the electric field across the shock - and this electric field is known to be highly structured and variable on all measured scales down to the electron scales[7]. Figure 2 demonstrates large amplitude, small-scale electric field spikes within the main shock transition. However, the role of such spikes and their variability requires electron-scale multi-point measurements of the 3D electric field together with larger-scale measurements to accurately determine the shock orientation, motion, and feedback processes.

Electron heating

Just as ion trajectories within the shock are affected by small scale electric field structures, so electron trajectories and small scale electric field structures are altered by the large scale shock profile, which is constantly varying as a result of reformation and ion dynamics. Very little is known about the effect of large scale shock variability on the formation, size and lifetime of small scale electric field structures, such as those illustrated in Figure 2, but without this knowledge, the 3D electric field structure, and final electron distribution functions, cannot be predicted. Moreover, it is the electrons themselves that support most of the overall cross-shock potential jump, so the electron dynamics and energy partition are strongly interlinked processes.

Of key importance is the nature of the electron motion: Magnetised or unmagnetised? Dominated by steady fields or high frequency fluctuations or turbulence? What is the feedback from the ion scales? Electrons with different energies or gyrophases may behave differently, requiring good coverage over the full range of velocity space.

Heavier ion species heating

Observations of heavier ions show that they are efficiently heated and accelerated at shocks. This is somewhat puzzling, since the main shock fields are self-consistently tuned to process the dominant momentum and energy carriers, which in the case of the solar wind are protons. The resolution of this puzzle almost undoubtedly requires some interplay between the electric fields (at small scales) and larger variations.

2.2.3 How do shock variability and reformation influence shock acceleration?

Internal variability

Supercritical shocks are fundamentally variable in time and space. They exhibit reformation, a quasi-periodic variation in the shock profile on scales comparable to the proton gyroradius. This results in a non-planar, and varying, shock profile, with important consequences for how particles are deflected, heated and accelerated. Computer simulations[9, 10] such as that shown in Figure 3 illustrate the difficulty faced by two, or even four, spacecraft trying to disentangle the overall structure and dynamics of the shock surface[9, 11].

The trajectory of an individual ion through the shock ramp is controlled by the instantaneous electric field that it encounters – but since this field is structured and variable, different ions follow markedly different trajectories. The number of ions reflected by the shock, which is directly related to the partition of energy problem, is known to vary (see Figure 4) but determining the feedback between that variability and the shock energy partition requires simultaneous multi-scale measurements.

This variability leads to many complex trajectories within the shock, some of which result in ions being ejected into the upstream plasma. There they seed the shock acceleration process and modify the upstream plasma conditions. A knowledge of the intricate feedback between very fine scale electric field structures and ion dynamics, and the re-

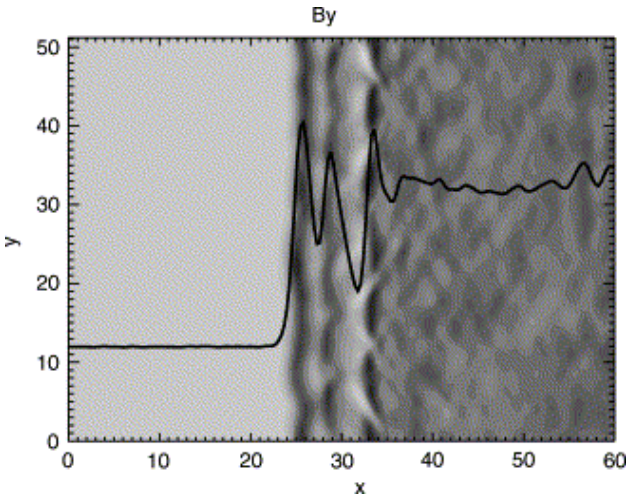

Figure 3: Two-dimensional magnetic field maps of a simulated shock. Note the structure and variability of the shock "surface." (from [10])

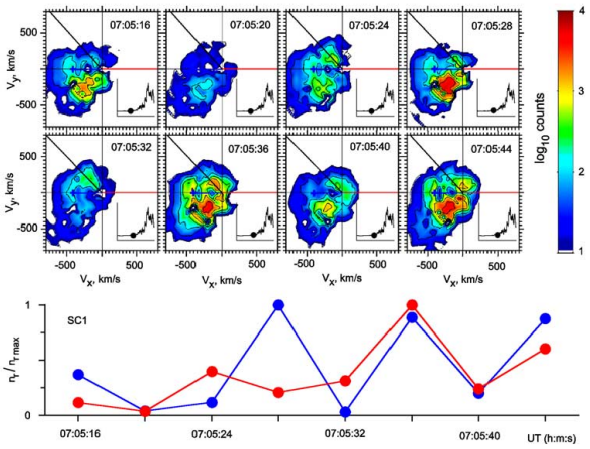

Figure 4: Ion distributions near the upstream edge of a high Mach-number shock (top) and the variability of reflected ions observed there (bottom). Quantitative assessment of the role of small scale fields, variability, and large scale control and consequences await full multi-scale measurements. (from [12])

sulting variability in the shock profile and structure, is essential for predicting the reflection and acceleration of ions around the shock, and in turn the bulk effect of shocks on the ambient medium.

Shock variability also has a strong influence on the acceleration of electrons. In the "fast Fermi process," incident electrons experience energy-gaining reflection that is a strong function of the angle between the magnetic field and local (on an electron scale) shock normal. Trapping within ripples and smaller variations enables electrons to reside close to the shock where they gain energy from the shock electric fields. Both these processes rely heavily on internal and variable shock structure.

Externally-induced variability

Several circumstances conspire to complicate the physics at real shocks. Some, described above, are intrinsic variability. Others are due to external variations which can have profound effects on the shock dynamics. For example:

Hot flow anomalies are formed when a plasma discontinuity with suitable orientation and parameters impinges on a shock front. Despite the overall pressure balance through such a discontinuity, and its thin structure, the particle dynamics at the interaction region can give rise to dramatic explosive events that create a hot cavity upstream of and/or attached to the shock. At the bow shock, these are observed to have some of the hottest, most thermalized particle distributions seen in situ anywhere in the solar system. It is not at all clear how particles are accelerated within the cavity and small scale magnetic field structures of a hot flow anomaly, nor the role played by electron dynamics. As sources of energetic particles and possible triggers of further events, these structures require further study. Measurements of the large, fluid-scale cavity shape and evolution must be made simultaneously with ion distributions within and around the cavity, as well as fine scale electric field and electron variations, in order to understand the dynamics and effects of these phenomena.

Shock-shock interactions occur often in real systems, such as travelling interplanetary shocks colliding with planetary bow shocks, or forward shocks catching up with slower or reverse travelling shocks in strongly variable astrophysical systems. Theoretically, such interactions provide conditions for extreme heating and particle acceleration, and will be studied in detail for the first time by Cross-Scale.

2.3 How does reconnection convert magnetic energy?

Magnetic reconnection is expected to occur when magnetic fields are sheared across relatively thin current layers[13]. In such current sheets the kinetic effects of the particle populations become important, and the onset of reconnection is expected to occur on the distance and time scales of the relevant electron and ion gyromotions. Microscale processes can control the change of topology of the magnetic field, eventually affecting the large-scale plasma mixing and converting magnetic energy to

plasma energy. On the other hand, large-scale (MHD) processes can control the location and formation of thin current sheets, and thus directly affect how reconnection initiates and evolves. It is therefore essential to follow both the large-scale and kinetic scale processes of the plasma to understand the onset, the evolution, and the result of the magnetic reconnection.

Current sheets where reconnection takes place can be either large scale boundaries, such as the Earth's magnetopause, tail neutral sheet, and solar wind discontinuities, or form dynamically on small scales, such as in magnetosheath turbulence (as shown in the Case Study on page 11) and within vortices at the magnetopause[14]. These regions include both strongly driven systems (such as the solar wind stand-off at the magnetopause) and relatively calm conditions (such as convecting solar wind current sheets).

The near-Earth plasma environment is unique in that we can make detailed measurements for different types of current sheets, including their formation and their microphysical processes. We can also examine in detail both the external conditions controlling the occurrence of reconnection and the large-scale consequences it has on the system. By simultaneously monitoring the essential scales, Cross-Scale will investigate the key questions in the reconnection as highlighted in the following subsections.

2.3.1 What initiates magnetic reconnection?

In order for magnetic reconnection to occur, a region must exist in which the magnetic field can diffuse relative to the plasma and across the current sheet separating two plasma regimes. Spacecraft observations suggest that this does not happen unless the shear angle between the magnetic fields either side of the boundary exceeds $\sim 70^{\circ}$. However, most current sheets for which that condition is satisfied remain stable much of the time, without any reconnection. Moreover, the conditions in the large scale plasma environments either side of reconnecting current sheets have been observed to be quite diverse, showing that reconnection is capable of happening under many conditions. We do not yet understand why reconnection begins, but an effective approach would be to study why it may begin at a particular point in a current sheet and not a neighbouring location. A basic requirement for making this comparison is numerous simultaneous measurement points both in and around a current sheet as it begins to reconnect.

According to present theory, a precondition for reconnection is that the current sheet must undergo a thinning process. Quantitative measurements of current sheet thinning have been made by the Cluster mission[20]. Cluster 4-point data can be used to determine the average current through the tetrahedron at a given moment. If the tetrahedron is small compared to a current sheet, a local measurement is made but the total current is unknown; if the tetrahedron is large compared to the sheet, the total current is measured, but its distribution within the sheet is unknown.

In order to fully characterise the development of thinning pre-reconnection current sheets we must therefore use a set of nested tetrahedra of spacecraft, across at least three scale sizes, each optimised to capture a different stage in the thinning process. The largest should give information about the magnetic flux gradient across the current sheet, and also characterise the orientation of the current sheet. The smaller ones should measure the intensification and thinning of current within the overall sheet structure, and also provide information on the internal variations in plasma characteristics to determine how such currents are supported. Nested tetrahedra provide more than three sets of 4-point data from which current can be calculated, providing valuable information about current and plasma substructures along and across the current sheet.

This set of multi-scale measurements will reveal the critical thickness at which a current sheet begins to break up. Measurements of ion and electron plasma properties put the critical thickness data into context in terms of the ion and electron scale sizes of the system, enabling ready comparison with analytical theory and simulations[21] (cf. Figure 5). Multi-point measurements of plasma waves and particle distributions will facilitate the testing of ideas about current sheet instabilities which may cause the breakup and initiate reconnection.

Internal current sheet instabilities may cause reconnection onset, but another possibility is the effect of an external driver. Both scenarios may be operating in different situations. Recent studies of magnetotail reconnection indicate that a large fraction of reconnection onset cases may be caused by sudden changes of the driving (global scale) electric field in the solar wind; similar suggestions have been made for magnetopause reconnection. Re-

Case Study: Reconnection in a turbulent plasma

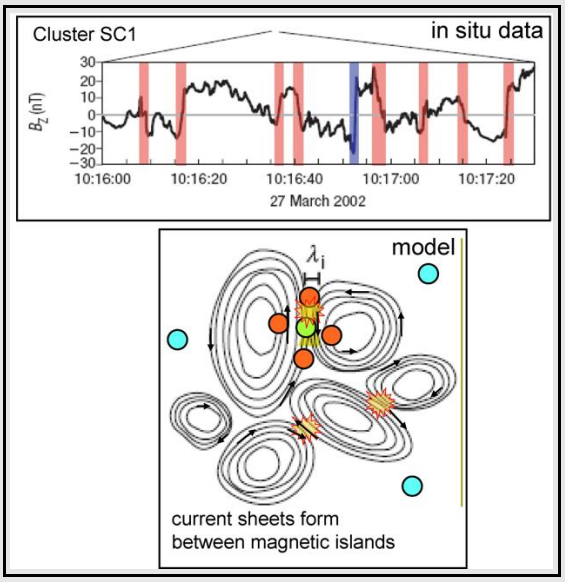

Magnetic reconnection has until recently only been observed at large-scale boundaries between different plasma environments. Observations analysed in [15] revealed, for the first time, in situ evidence of reconnection in a turbulent plasma. The turbulent environment is the magnetosheath, the solar wind downstream of the Earth's bowshock. The results have significant implications for laboratory and astrophysical plasmas where both turbulence and reconnection are common. The Figure shows observations of narrow current sheets in which reconnection takes place as well a schematic diagram, from numerical simulations[16, 17] that show the current sheet formation between coherent magnetic structures. Observations suggest that reconnection contributes significantly to particle energisation processes at the scales comparable to the small scales of current sheets or even smaller. However, much higher time resolution particle instruments and small separation spacecraft are required to understand particle energisation process at these small scales. At the same time, simultaneous observations of the largest scales are required to follow the evolution of coherent magnetic structures. The most recent studies already demonstrate that reconnection plays an important role in the development of turbulence, influencing intermittency and other properties[18].

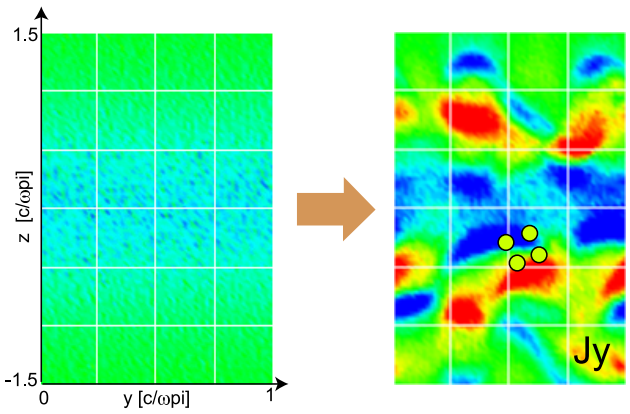

Figure 5: A simulation of a current sheet during the onset of a reconnection event[19]. The breakup of the current sheet is illustrated. A set of four electron scale Cross-Scale spacecraft is superimposed, to show how it would capture the transition from a stable sheet into rapidly changing fragmented currents which is thought to occur at reconnection onset. Additional spacecraft at larger separations will quantify the orientation and conditions in which that onset is triggered.

cently a set of simulations using various numerical schemes have investigated driven reconnection scenarios and show consistent outcomes, increasing confidence in the results. However, it is vital to make experimental tests of these results. As with the investigation of internal instabilities, this will require measurements within the current sheet on at least the ion and electron scales, and on the fluid scale outside the current sheet in order to capture the driver conditions.

2.3.2 *How does the magnetic topology evolve?*

Once magnetic reconnection has begun, there are many questions about how it is maintained. Reconnection in the solar wind can endure for hours[22]; at the magnetopause can be either similarly persistent or very bursty on a timescale of minutes; in the magnetotail reconnection seems more often to last only minutes or tens of minutes. However, these time scales are all long compared to typical electron and ion timescales, showing that reconnection can operate in a quasi-steady state, relative to the timescale of the kinetic processes that are thought to sustain it.

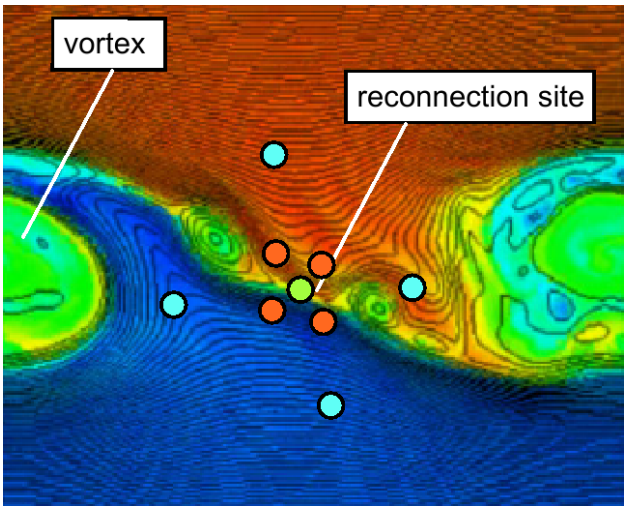

Figure 6: A simulation of a current sheet during a reconnection event. Note that the situation is more complex than the X-line scenario sketched in Figure 1. Such an ion/fluid scale simulation cannot simultaneously address the electron scale (for that, see Figure 5). A possible Cross-Scale configuration is superimposed showing how the large scale spacecraft measure the in/outflow jets and magnetic fields far from the current sheet; the intermediate/small scales are targeted on the ion/electron diffusion regions respectively.

Quasi-steady 2D reconnection

The most popular model of steady-state reconnection has anti-parallel magnetic fields either side of a current sheet. Plasma inflow and outflow vectors define a plane that is perpendicular to the current sheet and that also contains the anti-parallel magnetic fields (see the centre panel in Figure 7); the reconnection electric field is normal to this plane.

Magnetic reconnection occurs inside an electron diffusion region, which is very thin, with an extent normal to the current sheet of order an electro gyroradius or less (see Figure 5). This region is surrounded by an ion diffusion region no broader than an ion gyro-radius along the current sheet normal.

In their respective diffusion regions the ion/electrons are no longer magnetised, i.e. they no longer gyrate about the magnetic field and are not “frozen-in” to the magnetic flux. In the ion diffusion region, the reconnection electric field ensures that “frozen in” electrons continue to flow inwards towards the electron diffusion region but demagnetised ions are not affected in the same way. The electrons accelerate as the magnetic field weakens near the current sheet.

The relative motion of ions and electrons generates a “Hall current” directed against the inflow, and an oppositely directed “Hall electric field” acting to oppose the charge separation. A further consequence is that the electrons and magnetic flux are deflected out of the inflow/outflow plane, generating a characteristic quadrupolar “Hall magnetic field” signature.

In this picture, the electron diffusion region is somewhat of a “black box” and processes within it that demagnetise the electrons allowing reconnection to occur are not well understood.

We need comprehensive multi-scale measurements such as those proposed for Cross-Scale in order to validate this general picture and bring clarity to its grey areas. Single spacecraft observations have been interpreted as evidence of Hall magnetic fields, electric fields and outflow jets; these interpretations have been strengthened by 4-spacecraft multi-point Cluster observations showing that the fields and flows are organised in patterns consistent with expectations of this model. A more direct test for unmagnetised ions is needed to verify that the Hall fields are located within the ion diffusion region. This can only be accomplished by a comparison of the ion flow velocities and electric field drift velocities, which will differ there, set in their larger-scale context. Such a comparison requires very good plasma measurements and 3D electric field measurements. This test is an essential and unique Cross-Scale measurement.

The extents of the ion and electron diffusion regions are unknown, both along the external magnetic field direction and perpendicular to the 2D geometry (i.e., along the neutral- or X-line). They are vital to theoretical ideas about the reconnection rate and particle acceleration. These extents cannot be determined without monitoring the diffusion regions at electron/ion/fluid scales simultaneously. We need to be able to compare simultaneous observations from regions where reconnection is occurring, with nearby regions where it is not, in order to discover the factors which control the length of the neutral line.

Very little information is available about the electron diffusion region. In order to test ideas about how the diffusion occurs it will be necessary to measure the contribution to the reconnection electric field made by very small scale phenomena including non-gyrotropic electron pressure anisotropies or bulk electron flow anti-parallel to the main current. However, reliable data on particle be-

haviour in the electron diffusion region requires better time resolution than is available from today's research spacecraft[23]. In addition, we also need to identify any waves which may scatter and demagnetise electrons in and around their diffusion region. For example, whistler mode wave activity in the diffusion region may enable more efficient reconnection.

Departures from 2D

Reconnection topologies are most often more complicated than the picture discussed above; at the magnetopause, the large scale magnetic fields separated by the current sheet are often sheared, such that there is a component along the direction of the reconnection electric field. Many numerical simulations have studied how this "guide field" scenario might differ from the simpler 2D case, but this cannot be tested without multi-scale observations. Other departures from the symmetrical 2D picture that need to be examined include the differences in flow velocity, plasma density and temperature across the current sheet.

Cross-Scale measurements on all scales are needed to reveal whether there are differences in the way reconnection works at the magnetopause in comparison to the magnetotail. If so, are these to do with the electron scale, the ion scale or how they interact with each other and with the (asymmetric) driving at the fluid scale? Simulations suggest that reconnection is sensitive to the outermost boundary conditions of the system. Similarly, comparisons of magnetotail reconnection with and without significant oxygen ion populations are needed to test models of how the current sheet structure and reconnection rate depends on their plasma composition. It would be expected that an additional scale associated with oxygen gyroradii will play a role in controlling the reconnection process in this case.

Turbulent reconnection

The change in the magnetic topology due to reconnection is even more difficult to analyse within turbulent plasma regions. Turbulence can develop at plasma boundaries (such as vortices at the magnetopause[14]); changes in topology due to reconnection can lead directly to plasma transport across the boundaries and formation of the boundary layer[24] (see Figure 6). Thus spacecraft are required on a large scale to monitor the boundary layer development and on smaller ion/electron scales to understand the reconnection

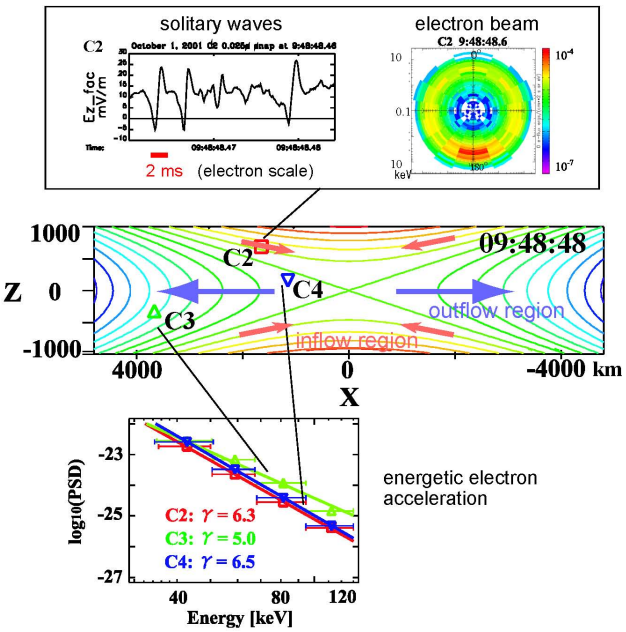

Figure 7: Electron acceleration within a reconnection region. Cold electrons are accelerated to keV energies by very small timescale (millisecond) interactions with electric field solitary waves[25]. Further acceleration to 100's keV involves non-adiabatic processes in the outflow region[26].

mechanisms (again here measurements must be made simultaneously on both ion and electron separation spacecraft).

In other situations, such as magnetosheath, the plasma is turbulent in a large volume; magnetic islands and other coherent magnetic structures can continuously form and disappear due to reconnection. The case study on page 11 illustrates one such example and also shows how Cross-Scale spacecraft at multiple scales are needed to analyse the reconnection in that case. Spacecraft at large separation would be able to follow the development of the turbulence while small separation spacecraft would be able to follow the physics of reconnection process itself. Both types of turbulent reconnection are expected in a wide range of astrophysical plasmas.

2.3.3 *How does reconnection accelerate particles and heat plasma?*

Reconnection most probably occurs in a wide variety of contexts beyond the Earth's magnetosphere; most can only be studied by remote sensing of the emissions generated indirectly by energetic particles. Even in the magnetosphere, energised particles measured in situ are often the only sign of a distant reconnection site. In order to interpret such

data as reconnection signatures or otherwise, and perhaps to use them to infer the properties of the reconnection site itself, we must understand how particles are accelerated and heated.

Most of the energy released during the reconnection process goes into the energisation of ions and electrons. Observations show evidence of reconnection outflow jets and particle heating, and of the formation of field-aligned beams and energetic tails in the particle distributions. However, their origin is not understood in detail.

Inductive electric fields associated with rapid changes in magnetic field may cause strong charged particle acceleration, such as in a reconnecting current sheet with a non-steady reconnection rate. To verify this with observations we need multiple spacecraft in the vicinity of the reconnection site to provide a combined data set that resolves space-time ambiguities and confirms that the magnetic configuration is rapidly varying. Local electric fields in 3-dimensions and particle data for a broad range of energies at high time resolution are needed to infer where in the system the acceleration occurs.

The reconnection electric field is expected to have a component along the local magnetic field direction in the diffusion region, which will readily accelerate charged particles[27]. A long neutral line can in principle accelerate particles to energies limited only by its length (e.g., 10's of keV in the magnetotail). A test of whether this acceleration mechanism really operates efficiently in nature requires a Cross-Scale constellation to make measurements of electric and magnetic fields, as well as particle populations, at several points along a significant portion of the length of a neutral line and around it. The upper part of Figure 7 shows data from a Cluster study which identified large amplitude electrostatic solitary waves seen only for milliseconds at the separatrices between in- and out-flowing material, together with a narrow 5 keV electron beam. The waves are consistent with an "electron hole" phenomenon predicted by simulations to occur in association with acceleration of inflow region electrons at the reconnection neutral line. Proper testing of this model requires simultaneous observations of this kind throughout the diffusion region and in the surrounding plasma.

Waves with a broad range of wavelengths and frequencies are generated in and around reconnection sites. Wave-particle resonant or diffusive interactions can both tap and enhance particle energy, with different wave types likely to affect different particle populations. Full characterisation of wavevectors and modes requires multipoint measurements on the corresponding scale. When analysing the gamut of relevant plasma waves, e.g., lower hybrid waves, whistler-mode waves, and electron cyclotron waves, we require separations simultaneously covering scales from tens of ions scales down to the electron scales. Confirmation of wave-particle interactions also requires well-resolved ion and electron velocity distributions at an appropriate cadence.

Strong wave activity is often reported in outflow jets, and energetic (100's keV) electrons are also often seen there, especially near the separatrices. One scenario for generating these electrons proposes that they are heated to a few 10's of keV near the reconnection site, and are further energised to 100's of keV by a combination of diffusion across the reconnection electric field together with strong pitch angle scattering that violates adiabatic invariants[28]. Betatron and Fermi acceleration are also expected on the contracting magnetic field lines in the reconnection outflow jets. Measurements on ion and fluid scales are needed to capture the evolution of particle energy with increasing distance away from the reconnection site, and to measure the magnetic field and other parameters to test whether the degree of energisation is consistent with that expected from these mechanisms. A partial example of such a test is seen in Figure 7 where three Cluster spacecraft located at increasing distances from the inferred diffusion region see electrons of progressively higher energies.

Significant fluxes of electromagnetic energy liberated at reconnection sites have also been observed to propagate away in the form of waves with an Alfvénic character. Their associated wave-particle interactions are known to cause local particle energisation. The generation mechanism of these waves is not clear. To make significant progress in understanding these waves and their relation to reconnection processes requires spacecraft that are suitably separated at several scales dictated by the nature of the waves: sub-ion scales to study the wave properties across the magnetic field, a few ion scales to study the environment of reconnection site and wave properties along the magnetic field and finally, hundreds of ion lengths

away along the magnetic field to see the development in the wave propagation.

2.4 How does turbulence control transport in plasmas?

The ubiquitous nature and important consequences of turbulence in space plasmas make it an important target for the Cross-Scale mission. Turbulence is responsible for the transport of many physical quantities: energy, both between scales and across space; momentum; and energetic particles through the resulting complex, tangled magnetic fields. It covers a vast range of scales, from inter-galactic to below the electron gyroradius.

While significant advances in simulation, theory and observations have been made, the highly complex, non-linear and multi-scale nature of plasma turbulence means that many important questions remain: How is energy transferred between scales, particularly at scales at which kinetic particle dynamics are important? How do the unique properties of plasmas alter the traditional hydrodynamic view of turbulence? What is the origin of the discrete structures that are observed in turbulent plasmas? All of these issues impact directly on the effects of turbulence on the surrounding plasma; without detailed knowledge of them we cannot predict the large scale effects of space plasma turbulence.

Cross-Scale offers a unique capability to address these fundamental questions about the nature and effects of turbulence in space plasmas. By measuring the 3D turbulent structure at three scales simultaneously, it will be possible for the first time to measure the energy transfer process as it actually occurs, at both fluid and kinetic scales. It will also sample plasma turbulence in a number of dramatically different regimes: the solar wind, where turbulence is well developed and energy inputs are steady; the highly disturbed magnetosheath, where fluctuations are highly driven by shocks and compressions; and the magnetotail, which is dominated by the magnetic field and therefore highly anisotropic.

The following sections describe key space plasma turbulence questions, and how Cross-Scale will address them.

2.4.1 How does the turbulent cascade transfer energy across physical scales?

Cascades, dissipation, and particle (non-fluid) scales

A defining characteristic of turbulence is the nonlinear transfer of energy between scales, a process that leads turbulence analysis to seek universal scaling laws. However, scaling laws can only exist where the energy transfer process is the same over a range of scales, such as within the plasma fluid (magnetohydrodynamic) regime. Some of the most important effects of turbulence, including plasma heating, particle scattering and the acceleration of stellar winds, are intimately related to fluctuations on the gyroscales of ions or electrons. On these scales, the turbulence is much more complex and is not scale invariant. In addition, many of the assumptions that are made to study fluid range turbulence, e.g., that the plasma flows past spacecraft much faster than the internal wave speeds, or that the plasma is incompressible, cannot be used: many more wave modes are present and they interact highly nonlinearly.

The four Cluster spacecraft have made it possible, using novel analysis techniques, to measure the wavevectors of turbulent energy in space plasmas for the first time[29]. However, this analysis is restricted to an order of magnitude in scales above the average spacecraft separation.

The small scale termination of the turbulence cascade is controlled by dissipation processes. While these are rather straightforward in collisional fluids where viscosity is dominant, in collisionless plasmas there are several possible mechanisms, on both ion and electron scales, and many wave modes, both electromagnetic and electrostatic, that can participate in the transfer of turbulent energy into particle heating. The multi-scale nature of this situation means that we have no satisfactory theoretical or observational understanding of it – and indeed it may be different in different plasma environments. However, without such a picture, we cannot hope to predict the effects of turbulent heating on space plasmas.

It is essential that the three physical scales of the cascade – fluid, ion and electron – are measured simultaneously with sufficient high quality instrumentation (electric and magnetic fields, ions and electrons) if we are to determine the properties of the active turbulent cascade. Cross-Scale,

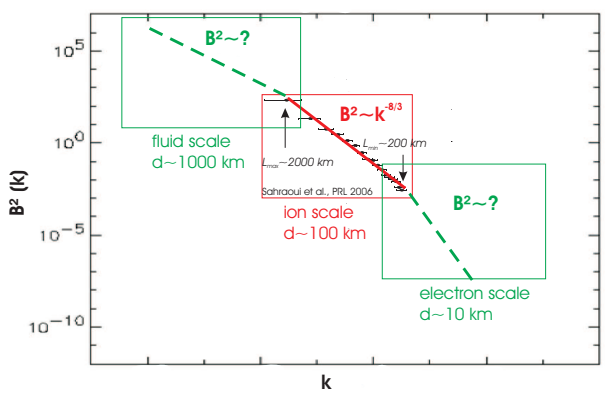

Figure 8: A wavevector spectrum of turbulent magnetic energy in the highly disturbed magnetosheath derived using multi-point measurements to filter the time series data into their joint space-time spectra. The fitted power law is shown in red for the range of scales, covering around a decade, which were accessible to the four Cluster spacecraft at this time. Electron and fluid scales, marked in green, would only be accessible at the same time with a three-scale formation mission such as Cross-Scale.

with its three tetrahedra targeted at these scales, will measure over this entire range for the first time (see Figure 8).

Theory suggests that in addition to the familiar energy cascade to small scales, a “reverse” cascade exists in quantities such as the magnetic helicity, making it possible to generate larger scale magnetic structures. However, such a cascade cannot be measured without multi-scale data. Cross-Scale will measure the helicity spectrum and its development, with the aim of identifying this reverse cascade for the first time.

Wave characteristics and particle interactions

Cross-Scale will not only measure turbulence over three decades of scale simultaneously, it will do so with highly targeted instrumentation. In particular, full ion and electron distribution functions will be measured at the relevant scales, as well as magnetic and electric fields. This will make it possible for the first time to track the energy flow from fluid to ion and electron scales and determine the direct effect on the particles themselves, such as resonances, wave generation and heating. Only in this way can we study the process by which turbulent energy is finally partitioned between fields and particles.

2.4.2 How does the magnetic field break the symmetry of plasma turbulence?

Neutral fluid turbulence is usually isotropic. Only near a boundary layer or other compression or shear is the isotropic symmetry broken so that turbulent properties become different in different directions. In contrast, the presence of a local magnetic field direction means that plasma turbulence is always anisotropic, even far from boundaries or shears. Indeed, theoretical work suggests that the turbulent cascade progresses differently parallel and perpendicular to the local field, a result that has been confirmed with spacecraft data in the solar wind[30].

Recently, multi-spacecraft data have made it possible to study anisotropy in the highly disturbed and turbulent plasma near the magnetopause boundary layer (see the Case Study on page 17). These reveal simultaneous anisotropies relative to two directions – the local magnetic field and the boundary layer – a scenario unique to plasma turbulence.

The anisotropy of plasma turbulence has important consequences for the transport of mass and energy through boundary layers. For instance, the velocity shear layer between the streaming solar wind and the stagnant magnetospheric plasma can become Kelvin-Helmholtz unstable and lead to highly anisotropic turbulent vortical flows, as revealed by recent 4-spacecraft Cluster observations. Structures with a scale comparable to the ion gyroradius can be created through cascading, or through secondary instabilities excited in the vortex. These small scale dissipative structures can mix the plasma contained in the vortex, and lead to diffusion through the shear layer.

The anisotropy of solar wind turbulence has important implications for the propagation of energetic particles throughout the solar system, as well as the large scale connectivity of the magnetic field: the turbulence can “braid” or tangle the magnetic field, resulting in field-line wandering far from the average direction (see the Case Study on page 17). These effects have been successfully used to reconcile scattering mean free paths of solar energetic particles with measured turbulence levels[30]. However, it is not clear how this anisotropy develops from the large scale where energy is injected, and how it passes between the fluid, ion and electron scales. In addition, the details of the energy transfer process itself are very poorly understood.

Case Study: Anisotropy and particle transport

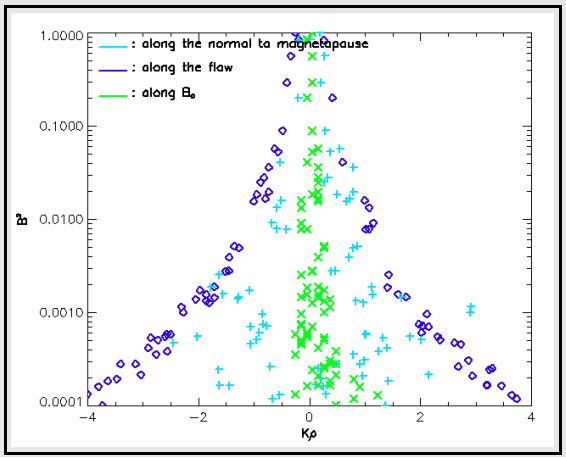

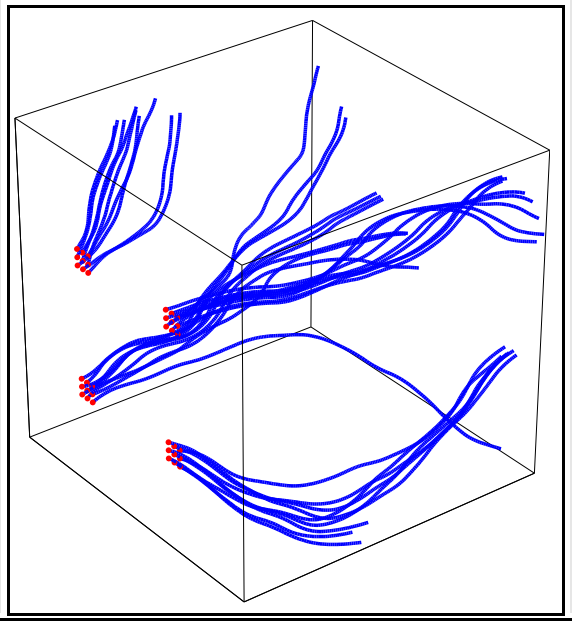

Measurements of turbulence in space plasmas have revealed the presence of significant anisotropy. Recently, multi-spacecraft data demonstrated that turbulence in the highly disturbed plasma downstream of the Earth's bow-shock scales differently in different directions[29] (see top figure). The power in wavevectors parallel to the field scales in a dramatically different way to that along the flow or perpendicular to the local plane of compression. This anisotropy appears to be due both to compression of the plasma next to the magnetopause boundary layer, and to the fundamental differences in energy transfer parallel and perpendicular to the magnetic field.

The anisotropy is of more than academic interest. Such anisotropy can have dramatic effects on the large scale connectivity of the magnetic field, as shown in the simulation box (bottom left), where field lines "wander" perpendicular to the field. The transport of energetic particles along this braided structure results in an enhanced diffusion process, which has important implications for the acceleration and propagation of, for example, cosmic rays, throughout the Universe.

Cross-Scale will make it possible to study for the first time how this anisotropy develops and is transferred between scales.

Cross-Scale will let us track the development of anisotropy between scales for the first time, providing information on how energy is transferred throughout space and time in the turbulent cascade. By relating this anisotropy to that observed in sheared or compressed hydrodynamic turbulence, we will gain insight into anisotropy as part of the universal process of turbulence. Recent advances based on the available data are limited to only around a decade in scale and at one location at a time, making it impossible to determine the evolution of anisotropy in scales or in space. Only Cross-Scale can make the multi-scale, multi-point measurements that are required, on both fluid and kinetic scales, to measure, understand and predict the effects of the anisotropy that is unique to plasma turbulence.

2.4.3 How does turbulence generate coherent structures?

In both neutral fluids and plasmas, turbulence generates discrete structures. Spacecraft data reveal the presence of large magnetic/density structures known as mirror modes[30, 31], Kelvin-Helmholtz waves[14] and current sheets[32], which appear to be involved in, or the result of, the energy transfer process. Fully-developed turbulence is generally not spatially uniform, and can exhibit strong spatio-temporal "burstiness," commonly known as intermittency (see Figure 9).

Intermittency has consequences on the transport of energy over scales, through the modification of the scaling in the inertial range, and on its dissipation at the small scales[33]. It is frequently proposed to explain the heating of the solar corona. It

is also expected to strongly affect scattering and diffusion of plasma particles[34]. Statistical methods brought from hydrodynamics (e.g., probability density functions and structure functions) have been applied to single spacecraft data but they cannot provide information on the 3D nature of intermittent structures in plasma turbulence.

Cross-Scale will make measurements at the fluid, ion and electron scales simultaneously, facilitating the analysis of the statistical properties of spatial and temporal inhomogeneity. That analysis will reveal how intermittency is generated and transmitted down the cascade. More than this, however, with Cross-Scale's 12 measuring points we will move beyond statistical analyses and for the first time actually "image" these structures, answering vital questions such as: How large are they? What is their 3D shape? How do they link together?

The recent identification of reconnection driven by turbulence (see the Case Study on page 17) demonstrates the importance of current sheets in turbulent flows. Their 3D structure and development is not well known, but without this knowledge we cannot predict the statistical effects of the resulting multiple reconnection sites. Additional observations of bursty reconnection in the Earth's magnetotail suggests that even in this very low β plasma, in which the strong magnetic field tends to resist the particle pressure, broad-band fluctuations can drive reconnection, emphasising the multi-scale nature of this process. These results show that turbulence and reconnection are intimately linked and a multi-scale approach is essential in order to fully quantify their effects.

Cross-Scale will not only measure three scales simultaneously: the 12 spacecraft formation can also be considered as multiple intermediate-scale tetrahedra at several locations. By performing a similar analysis at multiple locations simultaneously, for the first time it will be possible to measure unambiguously the growth and development of these structures as they travel past the formation.

2.5 Synergies with Other Science Endeavours

Cross-Scale (together with SCOPE) forms a stand-alone mission that addresses universal plasma processes. SCOPE is described further in Section 8.1. Modelling and simulational work will be an important contributor to all Cross-Scale science objectives. The capabilities and operations of the mission will provide numerous instances of synergy with other activities, some of which are described here.

Figure 9: A 2D simulation of electron MHD turbulence reveals that plasma currents are spatially localised into thin sheets and whorls. Many-point measurements, such as those from Cross-Scale, are required to measure such structures in 3D in space plasmas over a range of scales not accessible to simulation[35].

2.5.1 Magnetospheric physics

The availability of data from the outer magnetosphere provides a natural synergy with studies of the Sun-Earth coupling all the way to the ionosphere. Simultaneous global-scale observations will be made by networks of ground-based ionospheric radars, all-sky cameras, and riometers together possibly with satellite-borne imagers. Since magnetospheric regions map down to the ionosphere, those facilities gather a remotely-sensed 2D map that in effect adds a larger global scale context to the three fundamental scales covered by Cross-Scale. Thus global-scale measurements both enhance the multi-scale physics investigations and facilitate the exploration of their applicability, linking cause and effect, to the magnetosphere.

2.5.2 Interplanetary physics

At the other extreme, solar and interplanetary plasma measurements by spacecraft at the L1 Lagrange point, and elsewhere, extend observations of the drivers of the coupling processes to still

larger scales. Combinations of spacecraft at L1 and, for example, at the Moon, together with Cross-Scale will extend the study of turbulence to scales that approach those of source regions on the Sun.

2.5.3 Solar and astrophysical plasmas

As all of the plasma processes to be investigated by Cross-Scale are operating in more distant plasmas, the mission objectives are relevant to a very wide community. At the same time, interaction with that wider community will be essential to pose questions to the data, and phrase the resulting answers, in a way that is most accessible to scientists outside the core mission community.

2.5.4 Laboratory plasmas

Turbulence and reconnection are responsible for transport processes and disruption in laboratory plasmas, and form an important aspect of future experiments such as ITER. Thus Cross-Scale provides a vital incentive for these two relatively separate disciplines to cross-fertilise by addressing the physics rather than the context.

3 Mission Profile

Twelve spacecraft are required to observe simultaneously three disparate scales. This optimum configuration ensures that the measurements at each smaller scale are centred within their larger context. The payload demands at particularly the electron scale result in a spacecraft bus in the 100 kg class, with an overall dimension of $\sim$ 1.2 – 1.5 m. For reasons of economy, interchangeability, and operations, the multiple use of a single bus design is an effective strategy. Soyuz-Fregat launch capabilities can deliver 10 suitably-instrumented spacecraft into an Earth orbit where they can address the science objectives posed in Section 2; this forms the Cross-Scale ESA mission.

Cross-Scale's partner, the SCOPE mission to be provided by JAXA, complements the minimal configuration with (at least) two additional spacecraft, one with a comprehensive suite of high-resolution instruments that enhances the finely-targetted Cross-Scale capabilities at the smallest scales. SCOPE is described more fully in Section 8.1. The combination thus meets the optimal 12 spacecraft configuration with an optimal payload.

Table 2: Cross-Scale mass budget[36] incl. margin.

Item	No.	Mass* (kg)	P/L** (kg)	$\Delta V^{\dagger}$ (m/s)	Fuel (kg)
Fluid s/c	4	130	13	585	39
Ion s/c	4	156	39	235	17
Electron s/c	2	164	47	120	9
Dispenser	1	427		1215	1020
Total wet s/c		1713			
Tot. dispenser		1447			
Margin 23%		725			
SF-2 max.††		3885			

* Dry mass per item, includes payload
** Incl. ranging sys. + 23% average margin
† Includes de-orbit requirement
†† Soyuz-Fregat-2 (1b) to 20,000 km

3.1 Launch and Orbit

3.1.1 Overall Characteristics

The 10 ESA spacecraft will be accommodated on a single dispenser module, with the entire assembly launched using a Soyuz-Fregat 2 from Kourou. The launch mass budget is shown in Table 2. JAXA will provide a separate launch for SCOPE. The final apogee is of order 25 R_e with a low perigee (1.4 R_e geocentric). This roughly equatorial (14° inclination) orbit (see Figure 10) enables Cross-Scale to reach the regions where the targetted physics is occurring, including the dayside bowshock (12–20 R_e), reconnection at the magnetopause (8–12 R_e) and in the "tailbox" region of the geomagnetic tail (10–20 R_e), and turbulence in the solar wind (12-25 R_e), magnetosheath, and geomagnetic tail/plasma sheet. The orbit suffers a radiation dose of approximately 12 krad per year (assuming 4 mm of Al) and maximum eclipses of 8 hours. The mission can satisfy international space debris agreements through controlled de-orbiting of all spacecraft and the dispenser.

An alternative $10 \times 25\,R_e$ orbit would also meet the science objectives, but is difficult to reach within the launch capability for the 10 spacecraft configuration. A change in the number or size of spacecraft, or utilisation of additional launcher capacity (e.g., JAXA), could make such an orbit attractive in terms of both science and space debris control.

Payload mass estimates include intersatellite ranging systems ($\sim$ 5 kg) where needed. The payload mass margins on individual spacecraft, based on the instrument configurations summarised in Table 5, vary from 8% to 35%. The total payload mass carried by the 10 spacecraft (including ranging) is

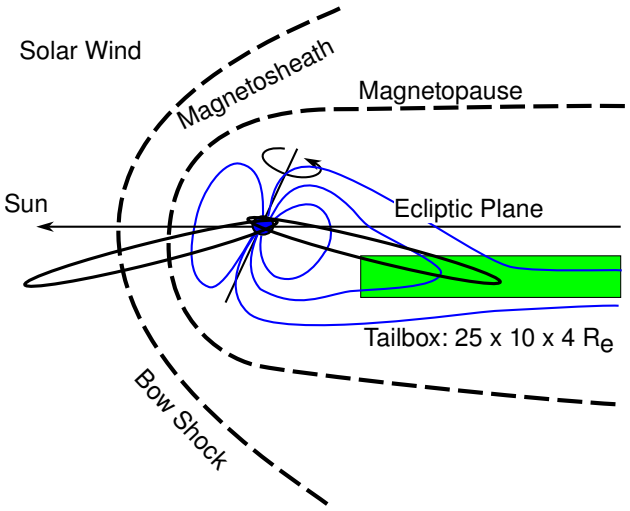

Figure 10: Cross-Scale orbit showing the location of the targetted regions. Note that the orbit precesses annually.

258 kg, to which a mass margin of 17% has been added to reach the total launch wet mass in Table 2; a further 23% margin has then been added to the final launch stack.

Propulsion requirements for deployment, constellation maintenance, and limited reconfiguration ranges from 10 m/s per spacecraft at the smallest scale, 125 m/s for the ion scales, and 475 m/s at the fluid scales[37]. These allow for corrections due to perturbations and drift. Masses in Table 2 include that required to de-orbit each spacecraft. A dispenser capable of delivering all 10 spacecraft to the high-apogee orbit is illustrated in Figure 11 with specifications given in Table 2.

The constellation of spacecraft will evolve around the orbit, essentially stretching out through perigee. All of the key science objectives are addressed with observations at interim to large geocentric distances, so that station-keeping can be kept to a minimum consistent with health and safety of the spacecraft and restricted operations resources. The constellation configuration is summarised in Table 3. In particular, the reconstruction of the spacecraft separation and relative timings between events observed on different spacecraft needs to be adequate to resolve the spatial and temporal variations on the scale of the different spacecraft separations. At the smallest, electron scale, these require dedicated spacecraft ranging systems. The baseline mission includes ranging on the ion scale spacecraft for accuracy and redundancy purposes.

Table 3: Constellation parameters and accuracy

Scale	Separation (km)	Accuracy	Timing (ms)
electron	2–100	125 m	0.25
ion	50–2000	1%	0.25–2
fluid	3000–15000	1%	2

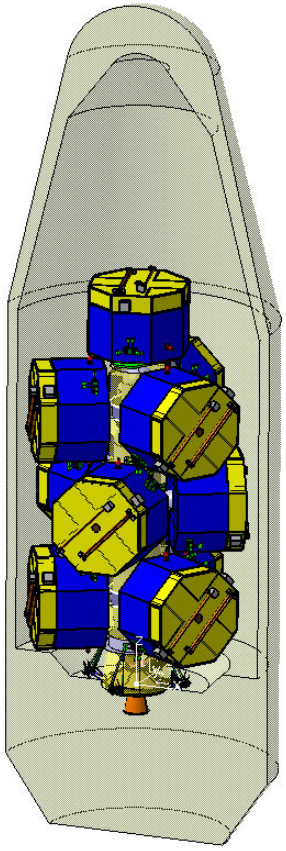

Figure 11: Dispenser vehicle with the 10 Cross-Scale spacecraft in their launch fairing[36].

3.2 Ground Segment

The ground segment is based on a minimal ESA Mission Operations Centre for commanding and occasional manoeuvres together with a Science Operation Centre that will coordinate instrument commanding and perform data handling and dissemination activities, including event identification and selection of data stored onboard for downlink the following orbit.

Comunication will utilise two existing ESA tracking stations, Perth and Maspalomas, equipped with 15 m antennas operating in the X-band. Each spacecraft will communicate directly with the ground station. There could be cost-benefit advan-

tages in S-band equipment which should be studied further. Shared ground segments with SCOPE and/or other international partners could be employed to increase the data return or possibly reduce overall costs. Data volumes and operations are discussed more fully below in Sections 4.3 and 6. Payload and spacecraft operations, and downlinks, need a high degree of autonomy to minimise the required ground segment resources.

3.3 Other Requirements and Issues

3.3.1 Orbit selection and mission lifetime

Final orbit selection will be agreed between the Cross-Scale and SCOPE elements. Commissioning and interspacecraft calibration will require 6 months followed by a nominal mission of 2 years. This will allow each of the relevant regions to be visited twice, permitting alternative spacecraft separation strategies/scales to be explored based on the science objectives and experience during the first year. This results in a total radiation dose of 30 krad.

3.3.2 Other agencies

Various possibilities exist to involve scientists and initiatives from other Agencies in the Cross-Scale concept. Examples are given below. These will need to be fully explored during the Assessment Phase. Letters of Commitment accompany this proposal.

Spacecraft provision

The Cross-Scale approach is scalable to incorporate additional spacecraft provided by new partners. These offer capabilities to enhance the range of scales and/or increase the coverage beyond the minimal four spacecraft at any particular scale. Such additions would be particularly helpful, and straightforward, at the fluid and larger scales. New partner missions could also provide complementary instrumentation and a level of redundancy to mitigate partial or total failure of a Cross-Scale spacecraft. Finally, should descoping be necessary, partner missions would be able to step in to complete the full multi-scale fleet. The current Cross-Scale/SCOPE launch capability could accommodate additional spacecraft (see Section 8.1).

Potential spacecraft-providers include Roscosmos, who have considered launching and deploying one or more spacecraft, and NASA. Other partners may also come forward during the Assessment Phase.

Instrument participation

Scientists from the USA have expressed an interest, through NASA, in participating in the mission at least at the level of payload. Similarly, Canadian scientists have coordinated potential involvement in flight hardware and science synergies. Given the substantial hardware to be flown, the resultant data volume to be analysed, and the contribution Cross-Scale can make to the science goals of many agencies, there are strong arguments to welcome the international aspects of the mission.

Ground-based systems and global imaging

Synergies in terms of magnetospheric physics exist between the Cross-Scale orbits and payload on the one hand and magnetospheric facilities on the other. The Canadian network of magnetometers, established in concert with NASA's Themis mission, would provide global coverage of the large-scale current systems and their dynamics, as would international radars (e.g., SuperDarn). Possible satellite-borne global imaging initiatives would enhance these diverse and complementary datasets. The Cross-Scale community includes scientists from all these disciplines.

4 Payload

4.1 Overview

The payload consists almost entirely of proven technology, with heritage in recent missions (e.g., Cluster, Polar, Themis, STEREO) and well-advanced concepts (e.g., MMS). Although the spacecraft bus and subsystems are identical, spacecraft devoted to different scales need different payload in terms of, e.g., time resolution, particle distributions vs. gross characteristics, and DC/AC fields. The largest demands come from the smallest scale (electron) spacecraft, with those at the fluid scale more modest.

To achieve this while benefiting from the economies of identical bus systems, the payload can be accommodated in universal mountings, such as modular bays or simple mounting plates. These plates present a common mechanical and electrical interface to the spacecraft, and are arranged on a single instrument shelf located at the top of the spacecraft. Figure 12 illustrates the concept, which provides ease of assembly, integration, and verification and facilitates replacement of faulty instruments. A thermal and electrical cover of some

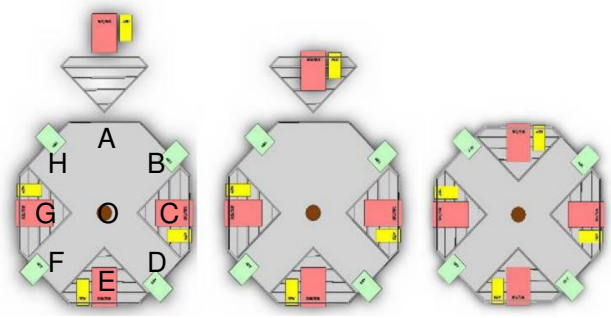

Figure 12: Instruments mounted on universal plates[36]. For reasons of economy, Cross-Scale will utilise a single spacecraft bus design. Since the science payload is not identical for all spacecraft, a modular approach is adopted to accommodate different instruments in the same position. For ease of assembly, integration, and verification, a universal plate will be provided to instrument teams. Plate locations used in Table 5 are lettered for convenience.

kind is needed, which could be a full or partial top to the entire spacecraft or specific to the individual bay.

Table 5 provides an overview of the instrument complement on each spacecraft, shown pictorially in Figure 13. The main spacecraft resources are provided in Table 6.

4.2 Instruments

The instrument complement on each spacecraft is targetted in terms of type of measurement, time resolution, and level of detail to match the highest science priorities (see [38] for details). The overall characteristics are shown in Table 4 with the deployment on the various spacecraft encapsulated in Table 5 and Figure 13.

DC magnetometers (dual-sensors) will be deployed on all spacecraft, returning field vectors sampled at up to ~ 100 Hz on the electron scale, and 1–10 Hz on the ion scale spacecraft. This data provides a robust roadmap of the 3D multi-scale morphology/connectivity, fundamental components of the overall turbulence spectrum, and specific fluctuations responsible for particle scattering and energisation.

AC search coil magnetometers extend waveform measurements up to ~ 500 Hz and spectral information up to several kHz. These complete the characterisation of waves responsible for particle scattering and extend the turbulence analysis into the electron dissipation range.

Electric field antennae will be used to cover the range from DC to 100 kHz on the inner spacecraft, where wave scattering and energisation of ions and electrons is a key priority for shocks and reconnection, and for the dissipation of turbulence. Electric measurements complement the magnetic ones to identify the electrostatic components of the waves and turbulence. The antennae will also be employed to measure the ambient DC electric field and the spacecraft floating potential. These, together with an **Electron density sounder**, provide a high time resolution, high quality total electron density measurement that is central to the shock and reconnection science objectives, and that underpins the calibration of the particle instruments. Apart from the fluid-scale spacecraft, all satellites will carry a crossed pair of wire boom antennae. At the electron scale all three components of the crucial reconnection electric field and the cross-shock electric fields will be completely characterised by the addition of rigid, dual-axial booms.

Electrostatic particle detectors of various designs will be carried on all spacecraft. These provide not only the basic plasma parameters (density, velocity, temperature, etc.) but also the full 3D velocity distribution functions. Collisionless plasma processes are driven by particle beams, temperature anisotropies, and other features that are not accessible to the low-order moments. Energy partition (heating and acceleration) amongst the various ion components requires some mass-resolving capability employing time-of-flight techniques in concert with the basic electrostatic design that is utilised for electrons. The comprehensive instrument suite on the SCOPE mother spacecraft (see Table 8) enables Cross-Scale to deploy a small number of core instruments to address the multi-scale aspects.

Modern analysers utilise a top-hat design which has a narrow field of view in one dimension. Full 3D velocity measurements require a full satellite spin period for a single sensor, which is adequate at the fluid scale. Multiple sensors, as either dual-heads within a single unit or multiple units, are deployed on the ion and electron scale spacecraft to increase the resolution and provide full 3D capability at the corresponding ion or electron time scales demanded by the science objectives. Additionally, deflector plates can be employed to increase the field of view for sub-spin resolution and reduce the number of sensors required. A combined electron/ion electrostatic analyser would greatly enhance the science return within payload mass restrictions by

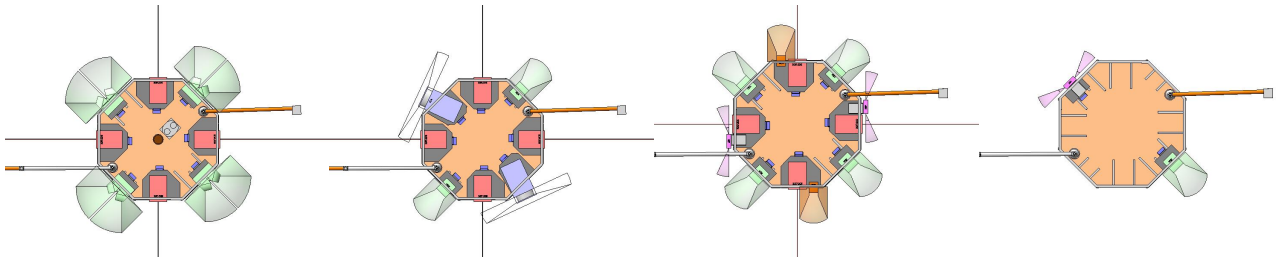

Figure 13: Accommodation and fields of view of the scientific payload on the electron (left), ion (two middle), and fluid-scale (right) spacecraft[36]. Table 5 identifies the instruments and bay locations, which are lettered in Figure 12.

Table 4: Cross-Scale Instruments - see Table 5 for key to the subset of these deployed on the different spacecraft

Instr	Mass* (kg)	Power* (W)	Volume** cm^3	Measurement	Recent Heritage	TRL
MAG	1.5	0.5	$11 \times 5 \times 5$ ($\times$2 units)	Boom-mounted DC vector magnetic field	VEX, Double Star	9
ACB	1.75	0.1	$10 \times 10 \times 10$	Boom-mounted AC vector magnetic field 1Hz–2kHz (spectra + waveform)	Themis, Demeter	9
E2D	8.0	3.0	$20 \times 30 \times 15$ ($\times$4 units)	30–50m wire double probe 2D electric field (DC + spectra) 0–100kHz (DC + spectra)	Themis, MMS, Demeter	8
E3D	4.0	2.0	10 cm dia.	Dual axial 5m antennae; (DC + spectra)	Polar, Themis	7
EDEN	0.2	0.25	-	electron density sounder	Cluster	9
ACDPU	1.5	2.0	$23 \times 19 \times 6$	Common processor & electronics for ACB, E2D, E3D, EDEN	Cluster	7
EESA	2.0	3.0	$26 \times 15 \times 26$	Dual-head thermal 3D electron electrostatic analyser 3eV–30keV	MMS	6
CESA	2.5	2.0	$15 \times 20 \times 15$	Combined 3D ion/electron electrostatic analyser 3eV–30keV ions,electrons	Medusa/Astrid	6
ICA	5	6	$25 \times 45 \times 25$	3D ion composition <40 keV	Cluster	8
ECA	1	0.5	$10 \times 15 \times 15$	3D energetic multi-species ion analyser 100 keV–1 MeV	STEREO	8
HEP	1.2	1	$15 \times 5 \times 15$	Solid-state high energy particle detector >30 keV	Themis, Demeter	9
CPP	3.0	2.0	$10 \times 20 \times 5$	Centralised payload processor	Themis, SpaceWire	5
ASP	1.9	2.7	$19 \times 16 \times 17$	Active potential control	Cluster, MMS	8

$*$ Total (all units); excluding most margins; excludes booms

$**$ Sensor volume only for MAG, ACB; MAG electronics $19 \times 16 \times 10$

avoiding separate instruments for each species.

Energetic ion and electron detectors are required to investigate acceleration processes. The larger gyroradii and scales associated with these particles implies that not all spacecraft need to be so equipped, and the deployment pattern shown in Table 5 represents a minimal configuration at each scale in a way which returns essential information on energetic ions, electrons, 3D ion velocity distributions, and ionic species.

Centralised onboard processing represents an attractive means of coordinating the payload, sharing (and hence reducing) resources. A dedicated **wave processor** has been successfully used in the past to coordinate common commanding, data taking, signal processing, and telemetry for electric and AC magnetic field instruments. A similar approach to particle instruments may be adopted. Alternatively, a distributed system taking advantage of modern communication and comput-

Table 5: Cross-Scale payload by spacecraft. Instrument locations are given by lettered bays, and shown in Figure 12; blanks indicate instruments not flown on that particular spacecraft.

Instr	Spacecraft/Location on which Deployed			
	electron	ion		fluid
	e 1-2	i 1	i 2-4	f 1-4
MAG	F	F	F	F
ACB	B	B	B	B
E2D	ACEG	ACEG	ACEG	
E3D	O			
EDEN	Z	Z	Z	
ACDPU	Z	Z	Z	
EESA	BDFH			
CESA		BF	BDFH	D
ICA		DH		
ECA			AE	
HEP			CG	H
ASP	O			
CPP	Z	Z	Z	Z

Z refers to internal electronics

ing capabilities, such as SPACEWIRE, will be studied during the assessment phase. There are obvious and significant mass savings to be gained by reducing or eliminating one or several instrument-dedicated data processing units. This strategy needs to be developed in tandem with the multi-instrument bays in the current spacecraft design.

Active spacecraft potential control will be flown on the electron scale. This limits the contamination of the electron measurements by photoelectrons of spacecraft origin, and enables the low energy population to be resolved without large and often uncertain corrections.

The basic characteristics of the instruments are described in Table 4. All instruments have recent flight heritage. Ongoing developments in mass, power, and science performance will be utilised to optimise the actual mission hardware.

4.3 Data rates

The science requirements met by the payload complement on the various spacecraft lead to a substantial data volume. That volume is estimated in Table 7, and used to allocate adequate spacecraft resources, telemetry, and ground station support.

The total mission data rate is 1.6 M-science words per second. A 16-bit science word (generous for the particle instruments) and a compression ratio of 10 (conservative given modern compression techniques for particle data, which dominates the data volume) would imply a mission data-rate of 2.6 Mbps of which 31% can be accommodated in a nominal total downlink capability of 800 kbs. The actual downlink budget is driven by the subset of the orbit corresponding to the key target regions and boundary layers, so the full science objectives can be comfortably accommodated by this data rate. In fact, the majority of the data volume is generated by the electron scale spacecraft. Based on Table 7, these accumulate roughly 61 Gbytes of compressed data in two orbits (6 days). If adequate centralised onboard storage is not available for these spacecraft, a number of strategies exist to avoid compromising the science, including internal instrument memory, autonomous or predicted event triggers, higher compression, and down-sampling in energy-angle-time resolution.

5 Spacecraft Considerations

5.1 Spacecraft Characteristics

For reasons of economy, all 10 spacecraft will share a common bus with instrument “bays” capable of accommodating different instruments as illustrated in Figure 12. The instrument suite on an individual spacecraft will target the appropriate key measurements for one physical scale (electron, ion, or fluid), with some limited redundancy between scales.

The spacecraft design [37, 36] is $\sim$ 1.5 m in diameter with a total dry mass (excluding payload) of $\sim$110 kg. AOCS is provided by combined sun and star sensors together with mono-propellant thrusters (bi-propellant systems have been considered, but existing flight-proven mono-propellant units offer similar overall performance and can provide the necessary levels of thrust). The spacecraft are spin-stabilised at 20–40 rpm. Faster spin-rates improve data resolution at the fluid scales, but at the electron scales stability of the spin-axis electric antennas limit the spin-rate to these values.

Intersatellite ranging is required on at least the electron scale spacecraft, and will be carried on the ion scale spacecraft to guarantee the accuracy demanded by the mission and to provide redundancy. This would utilise the X-band transponders, although a separate S-band system could be employed. This area will require close coordination with the SCOPE to ensure that compatible systems are flown on both missions.

The maximum science payload, excluding margins, that can be accommodated by the bus design

Table 6: Mass and power requirements of the payload complements on the different spacecraft, excluding margin.

	Mass (kg)	Power (W)	e 1-2 No.	Mass	Power	i 1 No.	Mass	Power	i 2-4 No.	Mass	Power	fluid No	Mass	Power
MAG	1.5	1	1	1.5	1	1	1.5	1	1	1.5	1	1	1.5	1
ACB	1.75	0.1	1	1.75	0.1	1	1.75	0.1	1	1.75	0.1	1	1.75	0.1
E2D	8	3	1	8	3	1	8	3	1	8	3	0	0	0
E3D	4	2	1	4	2	0	0	0	0	0	0	0	0	0
EDEN	0.2	0.25	1	0.2	0.25	1	0.2	0.25	1	0.2	0.25	0	0	0
ACDPU	1.5	2	1	1.5	2	1	1.5	2	1	1.5	2	1	1.5	2
EESA	2	5.5	4	8	22	0	0	0	0	0	0	0	0	0
IESA	1.5	2	0	0	0	0	0	0	0	0	0	0	0	0
CESA	2.5	2	0	0	0	2	5	4	4	10	8	1	2.5	2
ICA	5	6	0	0	0	2	10	12	0	0	0	0	0	0
ECA	1	0.5	0	0	0	0	0	0	2	2	1	0	0	0
HEP	1.2	1	0	0	0	0	0	0	2	2.4	2	1	1.2	1
CPP	3	2	1	3	2	1	3	2	1	3	2	1	3	2
ASP	1.9	2.7	1	1.9	2.7	0	0	0	0	0	0	0	0	0
Ranging	5	*	1	5	*	1	5	*	1	5	*	0	0	0
Totals			13	34.85	35.05	11	35.95	24.35	15	35.35	19.35	6	11.45	8.1

* Included in spacecraft system power budget

is 40 kg consuming 40 W[36]. Less mass is available on the ion and fluid spacecraft due to the additional fuel requirements. Each spacecraft will require a storage device of $\sim$ 256 Gbits to hold two full orbits of data; the two electron spacecraft will require additional storage within the EESA electronics and/or onboard selection algorithms (see Table 7). Communications will be direct to ground stations using an X-band transponder such as that baselined for GAIA. This provides variable datarates up to ~6.5 Mbps. Alternative low-mass systems are expected to become available in Europe in time to be considered for the mission.

5.2 Electromagnetic Cleanliness

Electromagnetic field measurements form a core part of the data from all spacecraft, and a comprehensive cleanliness programme, together with appropriate boom considerations, will be necessary to meet the science requirements. Previous mission experience shows that standard techniques to minimise noise through appropriate wiring strategies, judicious use of materials and parts, and rigid boom mounting of magnetic sensors will be adequate. Continuous surface conductivity will also be important to provide electrostatic cleanliness, enabling accurate measurements of low-energy particles to be made. In flight calibration and intercalibration will provide definitive characterisation of the stray DC fields and AC contamination.

6 Science Operations and Archiving

6.1 Spacecraft Operations

Operations will be centralised and, where possible, autonomous, e.g., in terms of instrument modes and data taking. The full dataset will be too large to transmit to ground. Data will be stored onboard each orbit, with a representative subset (e.g., everything except the highest resolution data from the electron scale spacecraft) telemetred to the Mission Operations Centre. The Science Operations Centre, which could be virtual or co-located at a science data centre, will use that data to select periods of interest with regard to the science objectives of sufficient duration to fill the downlink budget. Data from those intervals, from all spacecraft, will be telemetred during the next contact period(s).

A fallback automatic selection based on average locations of the boundaries and processes and the orbital position will be in place. Onboard event selection based on suitable triggers provides an alternative and reduces the onboard storage requirements.

The operation of 10 spacecraft, and the joint

Table 7: Cross-Scale data volumes

	Dim 1 E, comp	Dim 2 th, freq	Dim 3 phi	Dim 4 species	Time Stamp	e1-2 No.	Rate (Hz)	Vol Words/s	i 1 No.	Rate (Hz)	Vol Words/s	i 2-4 No.	Rate (Hz)	Vol Words/s	Fluid No	Rate (Hz)	Vol Words/s
MAG	3	1	1	1	1	1	100.0	400	1	100.0	400	1	100.0	400	1	50.0	200
ACB	3	1	1	1	1	1	500.0	2000	1	500.0	2000	1	500.0	2000	1	200.0	800
E2D (dc)	2	1	1	1	1	1	500.0	1500	1	50.0	150	1	50.0	150	0	10.0	0
E2D (ac)	2	32	1	1	1	1	100.0	6500	1	10.0	650	1	10.0	650	0	0.5	0
E3D (dc)	1	1	1	1	1	1	500.0	1000	0	50.0	0	0	50.0	0	0	10.0	0
E3D (ac)	1	32	1	1	1	1	100.0	3300	0	10.0	0	0	10.0	0	0	0.5	0
EDEN	1	1	1	1	1	1	500.0	1000	1	50.0	100	1	50.0	100	0	10.0	0
ACDPU	0	0	0	0	0	1	0.0	0	1	0.0	0	1	0.0	0	1	0.0	0
EESA	30	12	32	1	1	4	50.0	576050	0	10.0	0	0	10.0	0	0	0.5	0
CESA	30	12	32	1	1	0	50.0	0	2	1.0	11521	4	2.0	23042	1	0.5	5761
ICA	30	12	32	12	1	0	0.5	0	2	0.5	69121	0	0.5	0	0	0.5	0
ECA	30	12	32	12	1	0	0.5	0	0	0.5	0	2	0.5	69121	0	0.5	0
HEP	30	12	32	1	1	0	0.5	0	0	0.5	0	2	0.5	5761	1	0.5	5761
ASP	1	1	1	1	1	1	50.0	100	0	0.5	0	0	0.5	0	0	0.5	0
Data-rate: k-words/(s/c)/s								591.9			83.9			101.2			12.5
Total k-words/s/class								1183.7			83.9			303.7			50.1
Compressed Gbits/(s/c) in 2 orbits (6 days)								490.9			69.6			84.0			10.4
Total compressed Gbits in 2 orbits (6 days)								981.8			69.6			251.9			41.5

operations with JAXA, to appropriately position the spacecraft in the nested, multi-scale configuration is a challenge. However, ESA has ample experience in multi-spacecraft operations from which to evolve an effective strategy. The overall configuration is relatively stable; once it has been achieved, only minimal station-keeping will be required to compensate for any small drifts. The science objectives can be met without regular adjustments to the spacecraft separations; a single reconfiguration at the end of the first year of operations is planned to fine-tune the separation strategy in the light of the initial results.

6.2 Calibration

The large number of instruments will demand new approaches to instrument calibration activities. Preliminary calibrations will be performed on the ground to the extent possible, though it may be necessary and/or efficient to fully calibrate only a subset of each instrument type. Inflight intercalibration will be part of the commissioning phase, preferably while spacecraft are relatively close to others. Ongoing routine calibrations will require semi-autonomous procedures based on algorithms developed pre-flight and evaluated using existing multi-spacecraft datasets (e.g., Cluster) that have largely been calibrated using more labour-intensive methods.

6.3 Data Access

The mission will adopt a modern approach to data access, with the full dataset available to the Cross-Scale community, and open to the entire scientific community after a suitable delay (e.g., 6 months) to ensure adequate calibration and quality control. The Cluster experience of distributed data centres and an Active Archive will serve as a guide, but will form part of the mission concept from the outset. A lead role, e.g., at PI level, identified at the time of payload selection would provide the appropriate resource and schedule for coordination amongst the instrument teams and for the construction of the necessary software, standards, and data facilities.

7 Technology

The mission has no obvious technological obstacles. An ESA TRS [37] has confirmed its overall feasibility at mission, spacecraft, subsystem, payload, and operations levels. A follow-up industrial study [36] has provided further concepts and details that are largely consistent with the conclusions of the TRS.

7.1 Payload Readiness

Most, if not all, the instrumentation has sufficient heritage that it could be built and flown now without further development. Realistic instrument TRLs are given in Table 4. Improvements in mass and power requirements, increased autonomy, speed of duty cycle, and demonstrable multi-functionality

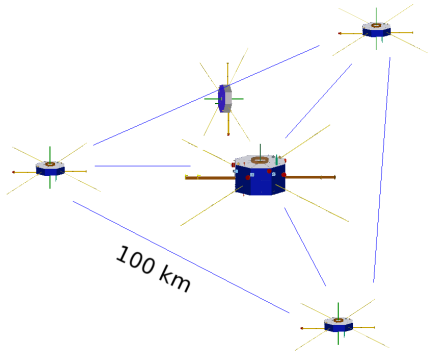

Figure 14: The original SCOPE concept: Mother, near daughter, and three intermediate daughters

(e.g., combined ion/electron detectors, capability for both hot and cold/solar wind ion distributions, etc.) will help to increase both the margins and the science return. Data compression, calibration and data processing are areas where efficiency will be paramount.

7.2 Mission and Spacecraft

No novel spacecraft engineering is required. Future studies will focus on the control and reconstruction of the interspacecraft positioning and synchronisation. This requires effective use of existing technology for intersatellite ranging. The dispenser module is based on existing commercial buses (SpaceBus 4000 or Eurostar 3000) and thus has a high TRL.

8 Programmatics and Costs

Cross-Scale will work in partnership with its sister mission, SCOPE, to be provided by JAXA. Below we summarise the characteristics of SCOPE before detailing the ESA cost estimates, alternative mission strategies, and risk management.

8.1 SCOPE

As noted in Section 3, the Cross-Scale/SCOPE combination not only meets the optimal 12-spacecraft configuration to fulfil the mission objectives, but also provides comprehensive high-resolution capability at the electron scale. SCOPE is a mature concept within JAXA. Its profile, payload, programmatics, and status are summarised below.

8.1.1 SCOPE Profile

The science objectives of SCOPE are closely aligned with those of Cross-Scale, addressing fundamental and universal plasma processes by using multi-point measurements to investigate the coupling between physical scales. Specifically, the mission objectives include magnetic reconnection, shocks in space, plasma mixing at boundaries, and the physics of current sheets[39]. The mission builds on JAXA/ISAS expertise in reconnection and associated turbulence investigated with GEOTAIL. The mother and a near daughter spacecraft are well-suited to studying the small scale electron processes within the tailbox region. The capabilities of the instrument suite have been designed to also study small-scale dayside phenomena (the bow shock, driven magnetopause reconnection, and turbulence).

The other three daughters, of comparable size to the Cross-Scale spacecraft, were designed to provide basic plasma parameters at intermediate (100–1000 km) scales to address the cross-scale coupling aspects of the key science objectives. The full complement continues to be under consideration by JAXA, but is dependent on the overall resources available for the mission. It is possible that up to two of the intermediate daughters may be constructed by JAXA.

At a minimum, the mother and near daughter would be provided by JAXA, with Cross-Scale completing and extending the multi-scale constellation. The spare launch capacity released by the removal of the three daughters could be used to launch two 150 kg spacecraft provided by international partners.

The mother payload is more ambitious than that accommodated by the Cross-Scale mission, and thus provides comprehensive and complementary datasets. Most notable are the intermediate energy particle instruments. The near daughter serves both to provide spatial information at very small (1–10 km) scales and, spinning orthogonal to the mother, employs long wire electric booms to capture, in combination with those of the mother, the 3D electric fields in a novel and totally unbiased way.

8.1.2 SCOPE Payload

The SCOPE payload is summarised in Table 8. Most of the instruments have heritage in previous missions or are in an advanced breadboard stage. The mother carries 87 kg of science payload and has a total dry mass of 464 kg. The near-daughter carries 14 kg of science payload with a total dry mass of 79 kg. An intersatellite ranging system is employed for accurate determination of space-

craft separation vectors (1% at separations down to 1 km); this would be integrated with a similar system on Cross-Scale at the electron scales.

8.1.3 SCOPE Launch and Operations

SCOPE will be launched on an H2A rocket from TNSC, Japan, either directly into a highly elliptical high apogee orbit or via GTO; both scenarios have been verified. The launcher is capable of delivering the complete SCOPE mission (including all daughters) into a high-perigee (9 R_e) orbit.

The studied orbit is inclined to spend approximately one month per year in the tailbox region (offset from the ecliptic to be placed within the reconnection regions) during winter. Cross-Scale mission requirements[37] are virtually identical. The mothership has hydrazine, bi-propellant, and mono-propellant systems for orbit insertion, manoeuvres, and attitude control; the daughter is equipped with mono-liquid hydrazine propulsion.

Communications will use X-band for both up- and downlink, with the intersatellite communications and ranging system operating in S-band. Ground segments are based on a 64 m dish at the Usuda Deep Space Center and a 34 m dish at the Uchinoura Space Center, both in Japan.

8.1.4 SCOPE Status and Schedule

SCOPE studies began in earnest in 2003; the concept is now mature. Key sub-systems, including intersatellite ranging, spin axis antenna design, and novel instruments have been under development since 2004; most of the science payload has strong flight heritage.

SCOPE will stay in Pre-Phase A for the next two years, during which the development of the Intersatellite Ranging and Clock Synchronisation System, spin axis antenna, and medium energy range particle spectrometers will be completed.

In late 2009, SCOPE will be reviewed by the Space Science Committee of ISAS/JAXA, after which it will move to Phase B. The earliest possible launch date is 2016 but this can be adjusted quite easily to match the Cross-Scale launch date in 2017.

8.1.5 SCOPE Budget

Assessment Phase

The budget for the Pre-Phase A term to the end of 2009 is guaranteed.

Cost to Completion

The total cost of the mission is estimated to stay within the envelope for a science mission managed by ISAS/JAXA.

8.2 Payload Provision

The number of spacecraft in Cross-Scale demands a large number of instruments, which following normal practice will be provided by the national agencies. This is feasible provided economies of mass production are fully exploited. A programme of streamlined ground calibration (plus in-flight intercalibration) will enable instruments to be delivered in a timely fashion.

8.3 Costs

The overall mission costs to ESA are shown in Table 10, based on ESA guideline amounts, estimates based on the study reported in [37], and estimates provided by industry. Two scenarios, of the several discussed in Section 8.4.2, are costed: a full implementation of the mission concept utilising the full 10 ESA spacecraft together with the mother-daughter SCOPE pair, and a minimal configuration comprising 6 ESA spacecraft together with 4 JAXA/other agency-supplied spacecraft.

We have estimated the costs to national agencies in providing the necessary instrument suites in Table 9. That table includes a salary element for scientists and technicians in the various laboratories although such costs are not explicit in the funding model employed in some countries.

Apart from the overall payload costs, the costs of non-ESA participants are not available. In particular, while the overall costs for SCOPE are not publically available, JAXA has confirmed that the mother, near daughter, and two intermediate daughters fit within the possible financial envelope.

8.4 Risks and Alternative Strategies

8.4.1 Risk Assessment

Cross-Scale is a relatively low-risk mission based largely on flight-proven technology and instrumentation. Operations and data processing will be challenging within a restricted set of resources, but manageable. The optimum mission includes the SCOPE elements to be provided by JAXA; a descope to 10 spacecraft in which one corner is shared by all three scales (electron, ion, and fluid) would meet the core objectives. Table 11 sets out the main risks and the mitigation strategy.

Table 8: SCOPE Payload Summary

Acronym	Instrument	Measurement characteristics
	Mother	
FESA	Fast electron spectrum analyser	10 eV–40 keV electrons (8 for ~2–8 ms resolution) @ 32×8×16
MESA	Medium energy electron spectrum analyser	2–100 keV electrons @ 1/2 spin @ 32 × 8 × 16
HEP-ele	High energy particles - electrons	3D electrons 30–700 keV @ spin
FISA	Fast ion spectrum analyser	5 eV/q–40 keV/q ions (4 for 1/8 spin resolution) @ 32×8, 32×16, 64
IMSA	Ion energy mass spectrum analyser	5 eV/q–25 keV/q ions @ 1/2 spin @ 32 × 8 × 16 for 8 masses in range 1-20
MIMS	Medium energy ion mass spectrum analyser	10–200 keV/q ions @ 1/2 spin @ 16, 32×8×16 for 5 masses
HEP-ion	High energy particles - ions	30–1000 keV 3D ions @ 12 energies @ 6 mass groups
MGF	Magnetic field	dual sensors mid- and tip of 5 m boom for vector magnetic field at 64,128 Hz
OFA/WFC-B	Onboard frequency analyser/ Wave-form capture - magnetic field	tri-axial search coil wave spectra and waveforms < 20 kHz
EFD	Electric field detector	30 m wire + 15 m tip-to-tip spin axis rigid dipole antennae for dc & low frequency electric field waveform and spacecraft potential
OFA/WFC-E	Onboard frequency analyser/ Wave-form capture - electric field	< 100 kHz electric field
HFR	High frequency receiver	single component electric spectrum 20 kH-10 MHz
DWPC	Digital wave-particle correlator	correlation index between plasma waves and particles
	Near daughter	
MGF		as for mother
EFD		as for mother
WFC-E		as for mother

Particle resolutions given in number of energy × polar × azimuthal bins.
Mother and daughter spin rate is 0.3 Hz

8.4.2 Alternative mission strategies

The mission objectives of simultaneous characterisation of the three key scales (electron, ion, and fluid) are uncompromisingly met by the full fleet of 10 ESA-supplied Cross-Scale spacecraft in partnership with the 2 (minimum) JAXA SCOPE spacecraft. In particular, this configuration enables measurements at each scale to be centred in the larger ones. The full context (e.g., upstream and downstream) in which the smaller scale is driven by, and feedbacks into, the larger scale is retrieved.

Nevertheless, for both financial reasons and in-flight spacecraft failure, it is important to assess the extent to which the science objectives could be addressed with fewer spacecraft, and to explore other scenarios. A subset of these is presented here, with the expectation that some will be explored in collaboration with any prospective partners during the Assessment Phase.

Eight ESA Cross-Scale spacecraft plus four SCOPE

This scenario retains the full science capability at reduced mass and cost to ESA. At this level, and especially in the further reduced scenarios described below, the mission relies on a firm ESA-JAXA partnership.

Ten ESA Cross-Scale spacecraft

In the event that SCOPE is unavailable, or fails, most of the ground-breaking science objectives could be met by configuring the 10 available spacecraft into a shared-corner configuration, as sketched in Figure 15. Some objectives, such as the acceleration and energy partition at shocks, could not be performed together as both the upstream and downstream regions would not be fully sampled. Thus reducing the total number of spacecraft to 10 requires more events for analysis, with

Table 9: Payload costs (M€) incl. staff

Instr.	Dev->EM	Per Unit	Num	Total
MAG	1.0	0.3	10	4.0
ACB	1.0	0.3	10	4.0
E2D	1.5	0.4	6	3.9
E3D	1.0	0.3	2	1.6
EDEN	0.2	0.1	6	0.8
ACDPU	0.5	0.3	10	3.5
EESA	3.0	0.5	8	7.0
CESA	3.0	0.5	18	12.0
ICA	3.0	0.5	2	4.0
ECA	3.0	0.5	6	6.0
HEP	2.0	0.3	10	5.0
CPP	0.5	0.3	10	3.5
ASP	2.0	0.5	2	3.0
Data Fac.	0.5	2.0	1	2.5
Totals	22.2		101	60.8

Table 10: Cross-Scale ESA mission costs

Full 10 spacecraft fleet

Activity	Cost M€	Margin %	Tot M€	Tot %
ESA study + internal	35	15	40	10
MOC and SOC	54	20	65	17
Industrial activities:				
s/c design to EM	30	10	33	9
s/c build	150	20	180	47
Dispenser	20	15	23	6
Soyuz Fregat-2B	39	10	43	11
Total	328	17	384	100

Minimum 6 ESA spacecraft

Activity	Cost M€	Margin %	Tot M€	Tot %
ESA study + internal	32	15	37	12
MOC and SOC	50	20	60	20
Industrial activities:				
s/c design to EM	27	10	30	10
s/c build	90	20	108	36
Dispenser	20	15	23	8
Soyuz Fregat-2B	39	10	43	14
Total	258	16	300	100

implications for the mission lifetime and more detailed constellation planning. Additionally, the more comprehensive instrument suite on the SCOPE mother would be unavailable. While this does not compromise the primary objective of cross-scale coupling, provided a core dataset as envisaged for the electron-scale spacecraft is available, it would have a measurable impact on the total science return.

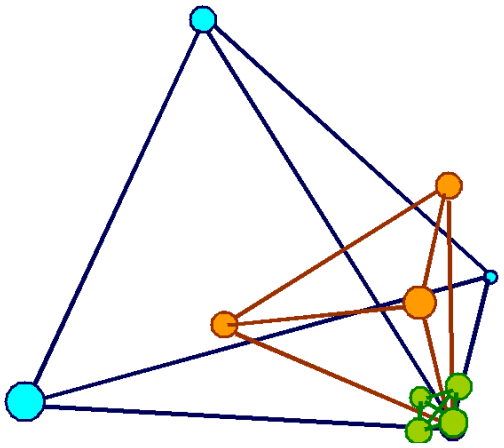

Figure 15: The shared-corner configuration for 10 spacecraft. This covers all 3 scales, but loses the context on one side.

Eight Cross-Scale spacecraft plus two SCOPE
Six Cross-Scale spacecraft plus four SCOPE

These scenarios would save ESA costs and launch mass. They would utilise the shared-corner configuration described above, with the benefit of the SCOPE instrument suite. Otherwise, they offer similar science capability and would meet the primary science objectives to a satisfactory level.

Eight Cross-Scale spacecraft
Six Cross-Scale spacecraft plus two SCOPE

With 8 spacecraft, 3D coverage of 3 scales is not feasible. However, it would be possible to cover two scales completely and hence to address the mission objectives by a sequence of constellations. A large fraction of the objectives require good understanding of the coupling between the ion and electron scales, and this coupling would be a priority in an 8-spacecraft mission. Turbulence studies and particle acceleration would benefit by some corner sharing here so that at least a single point at the fluid scale could be obtained simultaneously.

8.4.3 Options

The science objectives and mission concepts of Cross-Scale lend themselves well to creative and collaborative options which would save resource at the risk of adding international and operational complexity. While it is too early to lay down detailed

Table 11: Risk Assessment

Risk	Likelihood	Severity	Mitigation
ESA cost over-run	H	M	Descope to fewer ESA spacecraft; add international partner missions; use EM spacecraft as 10th; reduce redundancy (increases risk elsewhere); remove ion-scale ranging system
SCOPE unavailable	M	L	Put Cross-Scale in shared-corner configuration
National agency cost over-run	M	M	Widen international participation
National agency inability to fund full payload	M	M	Widen international participation
Single spacecraft failure	M	M	Adjust configuration to shared corner; add international partner missions for redundancy. Ensure minimal level of payload redundancy between different scales
Instrument failure	H	M	Ensure adequate payload redundancy between different scales
Instrument Development (e.g., Dual-head EESA, CESA with adequate geometrical factor)	M	L	Heritage instrumentation can be flown in place of any potential modified designs
Total mass excess	M	M	Some payload descope is possible which would affect secondary science goals; utilise SCOPE spare launch capacity; use low mass X-band system (lower TRL) or S-band
Science risk from alternative mission strategies	L	M	Evaluate science capability under alternatives; widen international participation

H = High; M = Medium; L = Low

scenarios, it is useful to know that they exist and should be considered if and when the need arises.

Dispenser and orbit

The dispenser that places the 10 Cross-Scale spacecraft into their near-final orbits needs sufficient subsystems to perform that task and then de-orbit itself from the nominal, low-perigee mission orbit. In fact, it needs power, communications, and AOCS. Two possibilities have emerged in a Cross-Scale industrial study[36]. One is to turn the dispenser into the 10th spacecraft to occupy one of the fluid-scale positions, say, by the addition of scientific payload, thereby making much better and longer use of the subsystems the dispenser must carry. Alternatively, use one of the 10 Cross-Scale spacecraft to provide the subsystems (power, communications) for the dispenser, which then is little more than a motor. The Cross-Scale spacecraft would then need to place the dispenser in an orbit that would decay and manoeuvre itself back to join the constellation.

Much of this is driven by the space debris requirement to de-orbit such low inclination, low perigee spacecraft. This also has implications for the fuel, mission lifetime, and reliability of all 10 Cross-Scale spacecraft. A higher perigee ($10\,R_e$) orbit would fully meet the science objectives, and would even be advantageous for studying driven reconnection at the magnetopause. Such an orbit does not appear to be reachable by the 10 Cross-Scale spacecraft on a Soyuz-Fregat launch vehicle. Moving some spacecraft to the daughter locations within the JAXA SCOPE launcher, or otherwise reducing the total launch mass, could enable the remaining ESA spacecraft to reach that higher perigee orbit, from which they and their dispenser would not need to de-orbit.

JAXA SCOPE daughters

The number of JAXA-built daughters in addition to the SCOPE mother-near daughter pair is under study. The original SCOPE mission included three such daughters; current estimates show that two would be feasible within the financial envelope. These would provide a comfortable level of redundancy for Cross-Scale and/or enable the overall Cross-Scale resource envelope to be reduced should that prove necessary (see Section 8.4.2).

Multi-agency collaborations

As noted in Section 3.3.2 there is already considerable international interest in the mission. That interest includes participation in the flight hardware and science objectives, which are well-aligned with those of many international space agencies.

Additionally, some agencies, such as Roscosmos or NASA, may be in a position to provide their own spacecraft. Depending on the size and scale, these would either be independently launched or possibly integrated into the SCOPE mission as daughter spacecraft.

Less redundancy/increased risk

The level of resource required is strongly dependent on the level of redundancy and reliability demanded.

9 Communications and Outreach

Cross-Scale is an ambitious undertaking targetted at quantifying fundamental, complex processes. The goal of any outreach programme should therefore capture the essence and universality of the key phenomena. The spacecraft will be studying shocks, reconnection, and turbulence within the near-Earth environment. Thus solar storms, geomagnetic activity, and their consequences (spectacular aurorae, telecommunications and technical systems outages, and bio-hazards) provide visual and tangible vehicles to convey the mission message. A familiar blend of web resources and media coverage will be employed.

References

[1] Schwartz, S. J. & Burgess, D. Quasi-parallel shocks - A patchwork of three-dimensional structures. *Geophys. Res. Lett.* **18**, 373–376 (1991).

[2] Giacalone, J., Schwartz, S. J. & Burgess, D. Observations of suprathermal ions in association with SLAMS. *Geophys. Res. Lett.* **20**, 149–152 (1993).

[3] Lucek, E. A. *et al.* Cluster magnetic field observations at a quasi-parallel bow shock. *Annales Geophysicae* **20**, 1699–1710 (2002).

[4] Burgess, D. *et al.* Quasi-parallel Shock Structure and Processes. *Space Science Reviews* **118**, 205–222 (2005).

[5] Yokoyama, T., Akita, K., Morimoto, T., Inoue, K. & Newmark, J. Clear Evidence of Reconnection Inflow of a Solar Flare. *Astrophys. J. Lett.* **546**, L69–L72 (2001).

[6] Kis, A. *et al.* Multi-spacecraft observations of diffuse ions upstream of Earth's bow shock. *Geophys. Res. Lett.* **31**, 20801 (2004).

[7] Walker, S., Alleyne, H., Balikhin, M., André, M. & Horbury, T. Electric field scales at quasi-perpendicular shocks. *Annales Geophysicae* **22**, 2291–2300 (2004).

[8] Bale, S. & Mozer, F. Measurement of large parallel and perpendicular electric fields on electron spatial scales in the terrestrial bow shock. *Phys. Rev. Letters* **in press** (2007).

[9] Burgess, D. Interpreting multipoint observations of substructure at the quasi-perpendicular bow shock: Simulations. *Journal of Geophysical Research (Space Physics)* **111**, 10210 (2006).

[10] Hellinger, P., Trávnícek, P. & Matsumoto, H. Reformation of perpendicular shocks: Hybrid simulations. *Geophys. Res. Lett.* **29**, 87–1 (2002).

[11] Moullard, O., Burgess, D., Horbury, T. S. & Lucek, E. A. Ripples observed on the surface of the Earth's quasi-perpendicular bow shock. *Journal of Geophysical Research (Space Physics)* **111**, 9113 (2006).

[12] Lobzin, V. V. *et al.* Nonstationarity and reformation of high-Mach-number quasiperpendicular shocks: Cluster observations. *Geophys. Res. Lett.* **34**, 5107 (2007).

[13] Biskamp, D. *Magnetic Reconnection in Plasmas* (Magnetic reconnection in plasmas, Cambridge, UK: Cambridge University Press, 2000 xiv, 387 p. Cambridge monographs on plasma physics, vol. 3, ISBN 0521582881, 2000).

[14] Hasegawa, H. *et al.* Transport of solar wind into Earth's magnetosphere through rolled-up Kelvin-Helmholtz vortices. *Nature* **430**, 755–758 (2004).

[15] Retinò, A. *et al.* In situ evidence of magnetic reconnection in turbulent plasma. *Nature Physics* **3**, 236–238 (2007).

[16] Dmitruk, P. & Matthaeus, W. H. Structure of the electromagnetic field in three-dimensional Hall magnetohydrodynamic turbulence. *Physics of Plasmas* **13**, 2307 (2006).

[17] Matthaeus, W. H. & Lamkin, S. L. Turbulent magnetic reconnection. *Physics of Fluids* **29**, 2513–2534 (1986).

[18] Sundqvist, D., Retinò, A., Vaivads, A. & Bale, S. Dissipation in turbulent plasma due to reconnection in thin current sheets. *Phys. Rev. Lett.* in press (2007).

[19] Tanaka, K. G., Shinohara, I. & Fujimoto, M. Parameter dependence of quick magnetic reconnection triggering: A survey study using two-dimensional simulations. *Journal of Geophysical Research (Space Physics)* **111**, 11 (2006).

[20] Nakamura, R. *et al.* Dynamics of thin current sheets associated with magnetotail reconnection. *Journal of Geophysical Research (Space Physics)* **111**, 11206 (2006).

[21] Daughton, W., Scudder, J. & Karimabadi, H. Fully kinetic simulations of undriven magnetic reconnection with open boundary conditions. *Physics of Plasmas* **13**, 2101 (2006).

[22] Phan, T. D. *et al.* A magnetic reconnection X-line extending more than 390 Earth radii in the solar wind. *Nature* **439**, 175–178 (2006).

[23] Henderson, P. D. *et al.* Cluster PEACE observations of electron pressure tensor divergence in the magnetotail. *Geophys. Res. Lett.* **33**, 22106 (2006).

[24] Fujimoto, M., Nakamura, T. K. M. & Hasegawa, H. Cross-Scale Coupling Within Rolled-Up MHD-Scale Vortices and Its Effect on Large Scale Plasma Mixing Across the Magnetospheric Boundary. *Space Science Reviews* **122**, 3–18 (2006).

[25] Cattell, C. *et al.* Cluster observations of electron holes in association with magnetotail reconnection and comparison to simulations. *Journal of Geophysical Research (Space Physics)* **110**, 1211 (2005).

[26] Hoshino, M. Electron surfing acceleration in magnetic reconnection. *J. Geophys. Res.* **110**, 10215 (2005).

[27] Drake, J. F., Swisdak, M., Che, H. & Shay, M. A. Electron acceleration from contracting magnetic islands during reconnection. *Nature* **443**, 553–556 (2006).

[28] Imada, S. *et al.* Energetic electron acceleration in the downstream reconnection outflow region. *J. Geophys. Res.* **112**, 3202 (2007).

[29] Sahraoui, F. *et al.* Anisotropic Turbulent Spectra in the Terrestrial Magnetosheath as Seen by the Cluster Spacecraft. *Physical Review Letters* **96**, 075002 (2006).

[30] Bieber, J. W., Wanner, W. & Matthaeus, W. H. Dominant two-dimensional solar wind turbulence with implications for cosmic ray transport. *J. Geophys. Res.* **101**, 2511–2522 (1996).

[31] Narita, Y. *et al.* Low-frequency wave characteristics in the upstream and downstream regime of the terrestrial bow shock. *Journal of Geophysical Research (Space Physics)* **111**, 1203 (2006).

[32] Knetter, T., Neubauer, F. M., Horbury, T. & Balogh, A. Four-point discontinuity observations using Cluster magnetic field data: A statistical survey. *Journal of Geophysical Research (Space Physics)* **109**, 6102 (2004).

[33] Frisch, U. *Turbulence. The legacy of A.N. Kolmogorov* (Cambridge: Cambridge University Press, 1995).

[34] Veltri, P., Zimbardo, G. & Pommois, P. Particle propagation in the solar wind: anomalous diffusion of magnetic field lines in turbulent magnetic fields. *Advances in Space Research* **22**, 55–58 (1998).

[35] Laval, J.-P. *http://www.atmos.ucla.edu/ ∼laval /Turbulence/ turbulence.html* (2007).

[36] EADS Astrium Ltd, UK. Cross-Scale: UK STFC-funded Study. *internal report* (2007).

[37] v den Berg, M. The Cross-Scale Technology Reference Study Documentation at http://sci.esa.int/ science-e/www/ object/ index.cfm?fobjectid=38982. *http://sci.esa.int/* (2007).

[38] The Cross-Scale Team. Cross-Scale Science Priority Document. *http:// www.cross-scale.org/ Documents/ CrossScaleSciPriorityDocV1.3a.pdf* (2007).

[39] Fujimoto, M. *et al.* The SCOPE mission. In Favata, F., Sanz-Forcada, J., Giménez, A. & Battrick, B. (eds.) *ESA Special Publication*, vol. 588 of *ESA Special Publication*, 249 (2005).

[40] Runov, A. *et al.* Current sheet structure near magnetic X-line observed by Cluster. *Geophys. Res. Lett.* **30**, 33–1 (2003).

[41] Vaivads, A. *et al.* Structure of the Magnetic Reconnection Diffusion Region from Four-Spacecraft Observations. *Physical Review Letters* **93**, 105001 (2004).

[42] Wygant, J. R. *et al.* Cluster observations of an intense normal component of the electric field at a thin reconnecting current sheet in the tail and its role in the shock-like acceleration of the ion fluid into the separatrix region. *Journal of Geophysical Research (Space Physics)* **110**, 9206 (2005).

List of Acronyms

EM	Engineering Model
GTO	Geostationary Transfer Orbit
ISAS	Inst. of Space Astronautical Sci. (Japan)
ITER	International Thermonuclear Experimental Reactor
JAXA	Japan Aerospace Exploration Agency
MHD	MagnetoHydroDynmaics
MMS	Magnetospheric Multi-Scale Mission
MOC	Mission Operations Center
R_e	Radius of Earth
SCOPE	Scale COupling in the Plasma universE
SOC	Science Operations Center
STFC	Sci. & Tech. Facilities Council (UK)
TNSC	Tanegashima Space Center
TRL	Technology Readiness Level
TRS	Technology Reference Study
VEX	Venus EXplorer

Image Credits

Cover Page top to bottom
- http://www.jhu.edu/news_info/news/home04/oct04/kepler.html
- NASA Marshall Space Flight Center
- Axel Mellinger, Univ. of Potsdam, Germany

Engineering diagrams EADS Astrium Ltd, UK

Other figures as cited in the text and/or by members of the Cross-Scale team

Cross-Scale Community

This proposal is submitted by the following 372 scientists from 23 countries.

Austria

Helfried K. Biernat
Kunihiro Keika
Stefan Kiehas
Werner Magnes
Rumi Nakamura
Andrei Runov
Klaus Torkar
Martin Volwerk
Tielong Zhang
Austrian Academy of Sciences

Manfred P. Leubner
University of Innbruck

Belgium

Fabien Darrouzet
Marius Echim
Johan De Keyser
Hervé Lamy
Viviane Pierrard
Michel Roth
Belgian Institute for Space Aeronomy

Giovanni Lapenta
Katholieke Universitei Leuven

Bulgaria

Emiliya Yordanova
Space Research Institute

Canada

Farbod Fahimi
Robert Fedosejevs
Sean Kirkwood
Ian R. Mann
Jonathan Rae
Robert Rankin
Illia Silin
Richard Sydora
Clare Watt
University of Alberta

Eric Donovan
Andrew Yau
University of Calgary

William Liu
CSA

Abdelhaq M. Hamza
Karim Meziane
University of New-Brunswick

China

Suiyan Fu
Zuyin Pu
Qiugang Zong
Peking University

Jinbin Cao
Chao Shen
State Key Laboratory for Space Weather/CSSAR

Xiaohua Deng
Wuhan University

Czech Republic

Ondrej Santolik
Zoltan Voros
Institute of Atmospheric Physics

Dana Jankovicova-Saxonbergova
Czech Academy of Science

Finland

Olaf Amm
Natalia Ganushkina
Tuija Pulkkinen
Finnish Meteorological Institute

Hannu Koskinen
University of Helsinki

Anita Aikio
University of Oulu

France

Gabriel Fruit
Vincent Génot
Philippe Louarn
Christian Mazelle
Henri Reme
CESR

Matthieu Berthomier
Patrick Canu
Gerard M. Chanteur
Thomas Chust
Olivier Le Contel
Dominique Delcourt
Dominique Fontaine
Bertrand Lembege
Raymond Pottelette
Laurence Rezeau
Alain F Roux
Fouad Sahraoui
CETP

Olga Alexandrova
Milan Maksimovic
LESIA

Thierry Dudok de Wit
Vladimir Krasnoselskikh
Aurélie Marchaudon
Jean-Louis Pincon
LPCE/CNRS

Germany

Joachim Saur
University of Cologne

Edita Georgescu
Stein Haaland*
Berndt Klecker
MPE-Garching
*also University of Bergen, Norway

Karl-Heinz Glaßmeier
Uwe Motschmann
Technische Universität Braunschweig

Joachim Vogt
Jacobs University Bremen

Jörg Büchner
Patrick W. Daly
Elena Kronberg
MPI für Sonnensystemforschung

Greece

Anastasios Anastasiadis
Olga Malandraki
National Observatory of Athens

Hungary

Peter Kovacs
Eotvos Lorand Geophysical Institute

Gabor Facsko
KFKI RMKI

Italy

Patrizia Francia
Massimo Vellante
Università di L'Aquila

Vincenzo Carbone
Antonella Greco
Gaetano Zimbardo
University of Calabria

Luca Sorriso-Valvo
INFM/CNR

Raffaella D'Amicis
Roberto Bruno
Maria Bice Cattaneo
Igino Coco
Giuseppe Consolini
Maria Federica Marcucci
Giuseppe Pallocchia
Istituto di Fisica dello Spazio Interplanetario - INAF

Thomas Penz
National Institute for Astrophysics

Japan

Koji Kondoh
Daisuke Matsuoka
Ken T. Murata
Tohru Shimizu
Masayuki Ugai
Kazunori Yamamoto
Ehime University

Takashima Asai
Tsutomu Nagatsuma
Institute of Information and Communications Technology

Kazushi Asamura
Masaki Fujimoto
Hiroshi Hasegawa
Hajime Hayakawa
Satoshi Kasahara
Kiyoshi Maezawa
Ayako Matsuoka
Takefumi Mitani
Yukinaga Miyashita
Toshifumi Mukai
Masato Nakamura
Takuma Nakamura
Masaki Nishino
Miho Saito
Yoshifumi Saito
Yoshitaka Seki
Nobue Shimada
Iku Shinohara
Taku Takada
Takeshi Takashima
Kentaro Tanaka
Takaaki Tanaka
Atsushi Yamazaki
Sho-Ichiro Yokota
Institute of Space and Astronautical Science

Ryoichi Higashi
Hisato Shirai
Ishikawa National College of Technology

Tooru Sugiyama
JAMSTEC

Yoshitaka Goto
Mitsuru Hikishima
Tomohiko Imachi
Yoshiya Kasahara
Isamu Nagano
Satoshi Yagitani
Kanazawa University

Kozo Hashimoto
Toshihiko Iyemori
Kaori Kaneda
Hirotsugu Kojima
Shinobu Machida
Hiroshi Matsumoto
Tomohiko Mitani
Yohei Miyake
Daisuke Nagata
Michi Nishioka
Naoto Nishizuka
Choosakul Nithiwatthn
Masahito Nose
Mitsuo Oka
Yoshiharu Omura
Akinori Saito
Kazunari Shibata
Tadahiro Shimoda
Koichi Shin
Naoki Shinohara
Mariko Teramoto
Yoshikatsu Ueda
Satoru Ueno
Hideyuki Usui
Hiroshi Yamakawa
Daiki Yoshida
Kyoto University

Shuji Abe
Akiko Fujimoto
Tohru Hada
Akihiro Ikeda
Yasushi Ikeda
Yoshihiro Kakinami
Hideaki Kawano
Shuichi Matsukiyo
Aoi Nakamizo
Yasuhiro Nariyuki
Takashi Tanaka
Teiji Uozumi
Akimasa Yoshikawa
Kiyohumi Yumoto
Kyushu University

Sachiko Arvelius
Yusuke Ebihara
Ryoichi Fujii
Akimasa Ieda
Yoshiko Koizumi
Junichi Kurihara
Yosuke Matsumoto
Yoshizumi Miyosh
Tetsuo Motoba
Akimitsu Nakajima
Nozomu Nishitani
Satonori Nozawa
Kaori Sakaguchi
Kanako Seki
Kazuo Shiokawa
Shin Tanaka
Takuo Tsuda
Taka Umeda
Tatsuhiro Yokoyama
Nagoya University

Shinsuke Imada
National Astronomical Observatory of Japan

Akira Kadokura
Yasunobu Ogawa
Masaki Okada
Yoshimasa Tanaka
Akira Yukimatsu
National Institute of Polar Research

Masao Nakamura
Osaka Prefecture University

Hitoshi Fujiwara
Yasumasa Kasaba
Atsushi Kumamoto
Hiroaki Misawa
Yukitoshi Nishimura
Takayuki Ono
Takeshi Sakanoi
Hiroyasu Tadokoro
Fuminori Tsuchiya
Manabu Yamada
Tohoku University

Masahiro Hoshino
Ichiro Yoshikawa
Kazuo Yoshioka
University of Tokyo

Yoshihiro Asano
Tsugunbu Nagai
Toshio Terasawa
Tokyo Institute of Technology

Keigo Ishisaka
Toyama Prefectural University

Mexico

Xochitl Blanco-Cano
Olivia L. Enríquez Rivera
Universidad Nacional Autonoma de Mexico

Norway

Nikolai Østgaard
Kristian Snekvik
Eija Tanskanen
University of Bergen

Jan A. Holtet
Bjørn Lybekk
Jøran Moen
Ellen Osmundsen
Yvonne Rinne
University of Oslo

Rico Behlke
University of Tromsoe

Poland

Jan Blecki
Barbara Popielawska
Roman Schreiber
Marek Strumik
Space Research Center of the Polish Academy of Sciences

Kris Murawski
UMCS

Romania

Adrian Blagau
Octav Marghitu
Institute for Space Sciences

Russia

Grigory Koinash
Anatoli A. Petrukovich
Sergey Savin
Oleg Vaisberg
Lev Zelenyi
IKI - Space Research Institute

Sergey Apatenkov
Victor A. Sergeev
St. Petersburg State University

Slovakia

Jozef Masarik
Comenius University

Karel Kudela
Jan Rybak
Slovak Academy of Sciences

Sweden

Lars Blomberg
Tommy Johansson
Tomas Karlsson
Per-Arne Lindqvist
Göran Marklund
Uwe Motschmann
Royal Institute of Technology (KTH)

Mats André
Jan E. S. Bergman
Stephan Buchert
Jonas Ekeberg
Anders Eriksson
Maria Hamrin*
Yuri Khotyaintsev
Tomas Lindstedt
Rickard Lundin
Hans Nilsson
Alessandro Retinò
Lisa Rosenqvist
Ingrid Sandahl
K. Stasiewicz
Gabriella Stenberg*
Andris Vaivads
Masatoshi Yamauchi
Swedish Institute of Space Physics
*also Umeå University

Taiwan

Motoharu Nowada
National Central University

Chio-Zong (Frank) Cheng
National Cheng Kung University

United Kingdom

William P. Wilkinson
University of Brighton

Mervyn Freeman
Richard B. Horne
Alan Rodger
British Antarctic Survey

Francois Rincon
Cambridge University

Chandrasekhar Reddy Anekallu
Yulia V. Bogdanova
Andrew Coates
Andrew Fazakerley
Claire Foullon
Paul Henderson
D. O. Kataria
Andrew Lahiff
Branislav Mihaljcic
Christopher J. Owen
I. Rozum
Yasir Soobiah
Andrew Walsh
University College London

Leah-Nani S. Alconcel
César Bertucci
Laurence Billingham
Chris Carr
Robert Forsyth
Edmund Henley
Tim Horbury
Bertrand Lefebvre
Elizabeth Lucek
Adam Masters
Alexander Schekochihin
Steve Schwartz
Anders Tjulin
Imperial College London

Mike Kosch
Patrick Daum
Michael H. Denton
Andrew J. Kavanagh
James Wild
Lancaster University

Sarah V Badman
Stanley W H Cowley
Robert Fear
Colin Forsyth
Carlos Gane
Adrian Grocott
Mark Lester
Steve Milan
Darren Wright
Tim Yeoman
University of Leicester

Emma E Woodfield
University of Liverpool

David Burgess
Queen Mary, University of London

Ruth Bamford
Robert Bingham
Jacqueline A. Davies
Malcolm W Dunlop
Mike Hapgood
Chris Perry
Rutherford Appleton Laboratory

Misha Balikhin
Yasuhide Hobara
Simon N. Walker
University of Sheffield

Mina Ashrafi
Betty Lanchester
Mike Lockwood*
Southampton University
*also STFC/Rutherford Appleton Laboratory

Andrew Buckley
Paul Gough
University of Sussex

Manuel Grande
University of Wales, Aberystwyth

Sandra C Chapman
University of Warwick

USA

Stuart D. Bale
Chris Chaston
Jonathan Eastwood
James McFadden
Marit Oieroset
Tai Phan
David Sundkvist
University of California - Berkeley

Vassilis Angelopoulos
University of California - Los Angeles

Stefan Eriksson
University of Colorado at Boulder

Katariina Nykyri
Embry-Riddle Aeronautical University

Melvyn Goldstein
Michael Hesse
Guan Le
Thomas E Moore
Antti Pulkkinen
David Sibeck
Jim Slavin
Timothy J Stubbs
Goddard Space Flight Center

Ken-Ichi Nishikawa
NSSTC - Huntsville

Karlheinz J. Trattner
Lockheed Martin ATC

Vania K. Jordanova
Benoit Lavraud
Geoff Reeves
Michelle F. Thomsen
Rob Wilson
Los Alamos National Laboratory

Terry Forbes
Harald Kucharek
Joachim Raeder
Roy Torbert
University of New Hampshire

James L Burch
Jerry Goldstein
Jörg-Micha Jahn
Dave McComas
Craig J. Pollock
South West Research Institute